Scientific African 29 (2025) e02769

Contents lists available at ScienceDirect

Scientific African

journal homepage: www.elsevier.com/locate/sciaf

A new generalization of power Chris-Jerry distribution with different estimation methods, simulation and applications

Mohammed Elgarhy [a,*], Diaa S. Metwally [b], Amal S. Hassan [c], Ahmed W. Shawki [d]

[a] Department of Basic Sciences, Higher Institute of Administrative Sciences, Belbeis, AlSharkia, Egypt
[b] Department of Accounting, Faculty of Business, Imam Mohammad Ibn Saud Islamic University (IMSIU), Riyadh 11432, Saudi Arabia
[c] Faculty of Graduate Studies for Statistical Research, Cairo University, 5 Dr. Ahmed Zewail Street, Giza, 12613, Egypt
[d] Central Agency for Public Mobilization & Statistics (CAPMAS), Cairo, Egypt

ARTICLE INFO

Editor name: B. Gyampoh

Keywords:
Transmuted-G family
Power Chris-Jerry distribution
Percentiles
Maximum product of spacing
Extropy measure

ABSTRACT

The choice of a suitable model has a major impact on the precision and dependability of statistical modeling results. A new model, the transmuted power Chris-Jerry distribution (Tr-PCJD), is presented in this study. The Tr-PCJD is a valuable generalization of the power Chris-Jerry distribution, known for its simplicity and effectiveness in modeling non-negative real-world. Its hazard rate function and density function support a wide variety of designs which reflects this adaptability. Additionally, it includes two existing models as well as a new sub-model. We examine the mathematical characteristics of the Tr-PCJD, such as random number generation, moments, and extropy measures, in order to highlight its significance. Along with that, we investigate eight estimation techniques for estimating the distribution's unknown parameters. The performance of the Cramer-von Mises, maximum likelihood, right tail Anderson–Darling, least squares, percentiles, Anderson–Darling, weighted least squares, and Anderson–Darling left tail second order estimators is assessed by an extensive simulation study. To further empirically validate the promise of the Tr-PCJD, we apply it to a real-world dataset.

Introduction

A fundamental tool for comprehending and evaluating real-world phenomena is a statistical distribution. Numerous lifetime applications call for more specialized models, even though classical distributions have been utilized extensively in disciplines like engineering, economics, finance, environmental research, and medicine. Scholars have investigated multiple strategies to generate novel classes of univariate continuous distributions that generalize existing distributions, with the aim of enhancing the adaptability of data modeling. The literature has put forth a number of created families; for a thorough summary, readers may consult Eugene et al. [1], Cordeiro and de Castro [2], Bourguignon et al. [3], Al-Shomrani et al. [4], Algarni et al. [5], Alghamdi and Abd El-Raouf [6], Eghwerido et al. [7], Hassan et al. [8,9], Afify et al. [10], Abdelall et al. [11], and Atchade et al. [12].

Shaw and Buckley [13] introduced the quadratic transmuted-generated (Tr-G) technique to add a new parameter τ, referred to transmuted parameter, to an existing distribution. A random variable Y is said to have the transmuted distribution if its cumulative distribution function (CDF) $F(y)$ and probability density function (PDF) $f(y)$ are given by

$$F(y) = G(y)\left[1 + \tau - \tau G(y)\right], \qquad y \in R, \ \ |\tau| \leq 1, \tag{1}$$

* Corresponding author.
E-mail addresses: dr.moelgarhy@gmail.com (M. Elgarhy), dmetwally@imamu.edu.sa (D.S. Metwally), amal52_soliman@cu.edu.eg (A.S. Hassan), ahmed23484@hotmail.com (A.W. Shawki).

https://doi.org/10.1016/j.sciaf.2025.e02769
Received 22 March 2025; Received in revised form 1 May 2025; Accepted 20 May 2025
Available online 4 June 2025

and

$$f(y) = g(y)\left[1+\tau-2\tau G(y)\right], \qquad y \in R, \ \ |\tau| \le 1, \tag{2}$$

where $G(y)$ is the CDF of the baseline model, $g(y)$ and $f(y)$ are the corresponding PDF associated with $G(y)$ and $F(y)$, respectively, and τ is the transmuted parameter. The Tr-G density is a mixture of the baseline density and the exponentiated-G density with power parameter two. It is significant to remember that the base random variable's distribution is presented at $\tau = 0$. Some generated distributions are produced by several authors [14–18].

Following a similar approach to the Lindley distribution (LD), the Chris-Jerry distribution (CJD), introduced by Ref. [19], is a one-parameter lifetime distribution that has gained increasing recognition. It was generated from a two-component mixture of gamma (3, η) and exponential (η) distributions, with a mixing proportion of $p = \eta/(\eta+2)$. Its superiority over numerous one-parameter competing distributions lies in the fact that it fits a wider range of data sets. Many applied fields require extended forms of the CJD. The development of these distributions in the statistical literature is relatively recent. Extended forms of CJD are Marshall–Olkin CJD [20], power size biased CJD [21], power CJD (PCJD) [22], Kumaraswamy CJD [23],shifted CJD [24], two-parameter CJD [25].

Our focus in this research is on a recently proposed, more flexible two-parameter lifetime model known as the PCJD, introduced by Ezeilo et al. [22]. It is considered as a generalization of the CJD with extra shape parameter. Its statistical characteristics have been thoroughly examined and several parameter estimate techniques have been investigated utilizing complete samples by Ezeilo et al. [22]. The PDF of the PCJD with the shape parameter $\kappa > 0$ and the scale parameter $\eta > 0$ is as follows:

$$g(y) = \frac{\kappa \eta^2 y^{\kappa-1} e^{-\eta y^{\kappa}} (\eta y^{2\kappa}+1)}{\eta+2}; \ \ y > 0. \tag{3}$$

The CDF and hazard rate function (HRF) of the PCJD are given, respectively, by:

$$G(y) = 1 - e^{-\eta y^{\kappa}} \left(\frac{\eta y^{\kappa}(\eta y^{\kappa}+2)}{\eta+2} + 1 \right); \ \ y > 0, \tag{4}$$

and

$$h(y) = \frac{\kappa \eta^2 y^{\kappa-1} (\eta y^{2\kappa}+1)}{\eta^2 y^{2\kappa} + 2\eta y^{\kappa} + \eta + 2}.$$

Often, the PCJD is not flexible enough to represent a variety of lifetime data well. To address this limitation, we propose a novel extension of the PCJD. Inspired by the Tr-G family, the new distribution, referred to as transmuted PCJD (Tr-PCJD), incorporates one additional parameter to enhance its modeling capabilities. The following goals are the focus of this study:

1. Create a flexible distribution that can represent uni-modal, reverse J-shaped, right-skewed, symmetric, and left-skewed can be seen in its PDF. A variety of shapes, such as increasing, J-shaped, declining, and reverse J patterns, can be seen in its HRF.
2. Investigate the key mathematical properties of the proposed distribution, including its moments, quantile function (QF), linear representation of the density function, incomplete moments (IMs), and extropy measures.
3. Estimate the unknown parameters of the Tr-PCJD using various estimation methods, including percentile estimation (PE), Anderson–Darling estimation (ADE), least squares estimation (LSE), maximum likelihood estimation (MLE), right-tail ADE (RTADE), Cramer-von Mises estimation (CVME), weighted least squares estimation (WLSE), and AD left-tail second order estimation (ADLTSE). To assess the performance of these estimators under different conditions, conduct a comprehensive simulation study.
4. Due to its flexibility, the Tr-PCJD emerges as a promising candidate for modeling three real-world datasets compared to existing alternatives. To demonstrate its superiority, this study investigates a range of contemporary statistical models, including XLindley distribution (XLD), Kumaraswamy LD (KwLD), Kumaraswamy CJD (KwCJD), Weibull power LD (WPLD), Weibull LD (WLD), exponentiated generalized XLD (EGXLD) and PCJD.

The following is the format of the paper: Section "Transmuted Power Chris-Jerry Distribution" presents the CDF, PDF, survival function (SF), and HRF of the Tr-PCJD. Section "Mathematical Characteristics of the Tr-PCJD" explores several structural aspects of the Tr-PCJD. Section "Estimation Methods" explores various estimation methods for the Tr-PCJD parameters and assesses the performance of different estimators using Monte Carlo simulation. Section "Applications" illustrates the practical applicability and versatility of Tr-PCJD through three real-world case studies. Finally, Section "Summary & Discussion" concludes the paper, summarizing the key findings.

Transmuted power Chris-Jerry distribution

This section derives the Tr-PCJD using the Tr-G family technique. We present expressions for its PDF, CDF, SF, and HRF. In addition, we provide graphical illustrations of the PDF and HRF, highlighting their various shapes.

The following expression represents the CDF of the Tr-PCJD, which is produced by substituting CDF defined in Eq. (4) with the CDF from Eq. (1):

$$F(y) = \left[1 - e^{-\eta y^{\kappa}} \left(\frac{\eta y^{\kappa}(\eta y^{\kappa}+2)}{\eta+2} + 1 \right)\right] \left[1 + \tau e^{-\eta y^{\kappa}} \left(\frac{\eta y^{\kappa}(\eta y^{\kappa}+2)}{\eta+2} + 1 \right)\right], \quad y > 0, \ \eta, \kappa > 0, \ |\tau| \le 1. \tag{5}$$

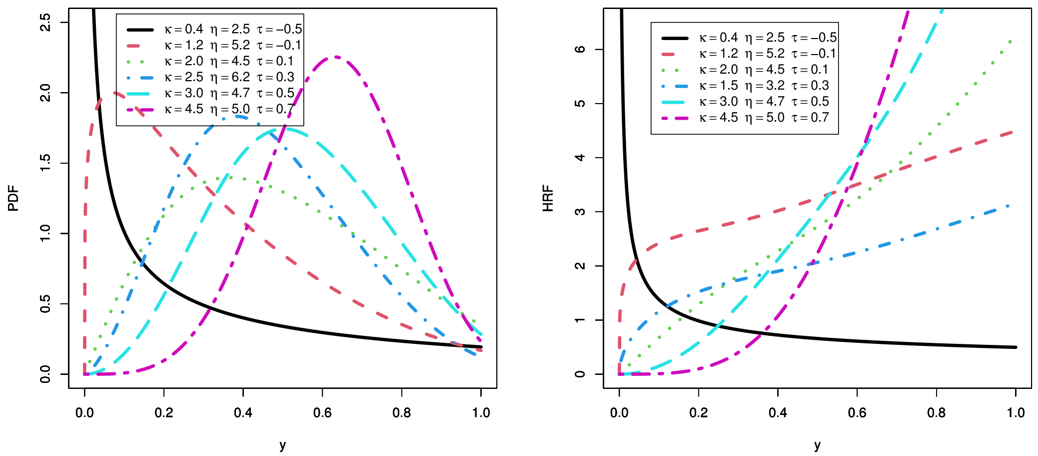

Fig. 1. Plots of the PDF and HRF for the Tr-PCJD.

The PDF of the Tr-PCJD is derived by substituting Eqs. (3) and (4) into Eq. (2)

$$f(y) = \frac{\kappa\eta^2 y^{\kappa-1} e^{-\eta y^\kappa}(\eta y^{2\kappa}+1)}{\eta+2}\left[1-\tau+2\tau e^{-\eta y^\kappa}\left(\frac{\eta y^\kappa(\eta y^\kappa+2)}{\eta+2}+1\right)\right], \qquad y>0,\ \eta,\kappa>0,\ |\tau|\le 1. \tag{6}$$

To demonstrate the flexibility of this PDF, we consider two special cases. When $\tau = 0$, it reduces to the CDF of the PCJD with parameters $\eta > 0$, and $\kappa > 0$ (see [22]). When $\tau = 0$, and $\kappa = 1$ the CDF becomes that of CJD with parameters $\eta > 0$ (see [19]). Finally, when $\kappa = 0$ we obtain the CDF of the transmuted CJD (Tr-CJD) with parameters $|\tau| \le 1$ and $\eta > 0$ as a new model.

The SF and HRF of the Tr-PCJD are specified by:

$$S(y) = 1-\left[1-e^{-\eta y^\kappa}\left(\frac{\eta y^\kappa(\eta y^\kappa+2)}{\eta+2}+1\right)\right]\left[1-\tau e^{-\eta y^\kappa}\left(\frac{\eta y^\kappa(\eta y^\kappa+2)}{\eta+2}+1\right)\right],$$

and

$$h(y) = \frac{\kappa\eta^2 y^{\kappa-1}e^{-\eta y^\kappa}(\eta y^{2\kappa}+1)\left[1-\tau+2\tau e^{-\eta y^\kappa}\left(\frac{\eta y^\kappa(\eta y^\kappa+2)}{\eta+2}+1\right)\right]}{(\eta+2)\left\{1-\left[1-e^{-\eta y^\kappa}\left(\frac{\eta y^\kappa(\eta y^\kappa+2)}{\eta+2}+1\right)\right]\left[1-\tau e^{-\eta y^\kappa}\left(\frac{\eta y^\kappa(\eta y^\kappa+2)}{\eta+2}+1\right)\right]\right\}}.$$

Fig. 1 illustrates the flexibility of the Tr-PCJD distribution by plotting its PDF and HRF for various fixed values of τ, η, and κ. These plots demonstrate a wide range of curvatures, including left-skewed, right-skewed, near-symmetrical, and reverse J shapes for the PDF, and increasing, decreasing, and upside-down bathtub shapes for the HRF. This versatility distinguishes the Tr-PCJD, making it well suited for modeling a diverse range of real-world datasets.

Mathematical characteristics of the Tr-PCJD

This section investigates several statistical properties of the Tr-PCJD distribution. We commence by deriving the quantile function (QF) and providing numerical examples. Subsequently, we explore other key characteristics, including moments, incomplete moments (IMs), Bowley's skewness, Moor's kurtosis, and specific extropy measures.

Quantile function

The QF is a valuable statistical tool that is used to determine the mathematical properties of a distribution and identify specific percentiles. It is essentially the inverse function of the CDF. For Tr-PCJD, the QF, denoted as $Q(u)$, can be expressed as $Q(u) = G^{-1}(u), 0 < u < 1$. It takes the following form

$$\frac{(\eta+2)\left(1+\tau+\sqrt{(1-\tau)^2+4\tau u}\right)}{2\tau} = e^{-\eta y^\kappa}\left(\eta y^\kappa(\eta y^\kappa+2)+\eta+2\right). \tag{7}$$

By solving the non-linear Equation (7), for y^κ, the solution gives the complete proof of QF of Tr-PCJD. For $u = 0.25$, 0.5 and 0.75 in Eq. (7) then Q_1, Q_2 and Q_3 are produced. Bowley's skewness (β_1) and Moor's kurtosis (β_2), on the other hand, give important details on the skewness and kurtosis of the Tr-PCJD based on the quantiles. The β_1 and β_2 are defined, respectively, by:

$$\beta_1 = \frac{Q(0.75)-2Q(0.5)+Q(0.25)}{Q(0.75)-Q(0.25)},$$

Table 1
Results of Q_1, Q_2, Q_3, β_1, and β_2 linked to the Tr-PCJD.

τ	κ	$\eta = 0.2$					$\eta = 0.6$				
		Q_1	Q_2	Q_3	β_1	β_2	Q_1	Q_2	Q_3	β_1	β_2
0.5	2.4	2.1228	2.6299	3.1389	0.0018	1.2776	1.1634	1.5535	1.9131	−0.0406	1.2763
	2.6	2.0034	2.4414	2.8745	−0.0056	1.2799	1.1499	1.5017	1.8200	−0.0500	1.2825
	2.8	1.9064	2.2906	2.6657	−0.0121	1.2821	1.1385	1.4587	1.7438	−0.0580	1.2880
	3.0	1.8261	2.1675	2.4970	−0.0176	1.2843	1.1287	1.4225	1.6803	−0.0652	1.2933
	3.2	1.7587	2.0652	2.3582	−0.0225	1.2863	1.1202	1.3915	1.6267	−0.0712	1.2981
	3.4	1.7012	1.9789	2.2421	−0.0267	1.2882	1.1127	1.3647	1.5808	−0.0766	1.3026
	3.6	1.6517	1.9053	2.1438	−0.0306	1.2898	1.1061	1.3414	1.5411	−0.0815	1.3067
	3.8	1.6087	1.8417	2.0595	−0.0340	1.2916	1.1003	1.3208	1.5064	−0.0857	1.3104
	4.0	1.5709	1.7863	1.9864	−0.0371	1.2931	1.0950	1.3025	1.4759	−0.0896	1.3139
	4.2	1.5375	1.7377	1.9225	−0.0399	1.2945	1.0903	1.2862	1.4488	−0.0930	1.3175
	4.4	1.5077	1.6946	1.8662	−0.0424	1.2961	1.0861	1.2716	1.4246	−0.0962	1.3205
	4.6	1.4810	1.6562	1.8163	−0.0448	1.2972	1.0821	1.2584	1.4028	−0.0993	1.3233
	4.8	1.4570	1.6217	1.7717	−0.0469	1.2984	1.0786	1.2464	1.3832	−0.1018	1.3259
	5.0	1.4352	1.5907	1.7316	−0.0488	1.2995	1.0753	1.2355	1.3653	−0.1043	1.3285
0.8	2.4	2.0257	2.5066	2.9719	−0.0166	1.2811	1.0852	1.4621	1.7976	−0.0580	1.2621
	2.6	1.9186	2.3355	2.7331	−0.0238	1.2844	1.0784	1.4200	1.7183	−0.0675	1.2690
	2.8	1.8314	2.1982	2.5436	−0.0301	1.2874	1.0726	1.3848	1.6532	−0.0756	1.2752
	3.0	1.7590	2.0858	2.3901	−0.0355	1.2903	1.0676	1.3551	1.5987	−0.0826	1.2810
	3.2	1.6980	1.9921	2.2635	−0.0403	1.2929	1.0632	1.3296	1.5525	−0.0889	1.2865
	3.4	1.6459	1.9130	2.1573	−0.0445	1.2953	1.0594	1.3075	1.5128	−0.0944	1.2914
	3.6	1.6010	1.8453	2.0671	−0.0483	1.2975	1.0560	1.2882	1.4784	−0.0993	1.2960
	3.8	1.5618	1.7867	1.9896	−0.0515	1.2995	1.0530	1.2711	1.4483	−0.1037	1.3001
	4.0	1.5274	1.7356	1.9223	−0.0546	1.3014	1.0503	1.2560	1.4217	−0.1075	1.3042
	4.2	1.4969	1.6906	1.8634	−0.0573	1.3033	1.0478	1.2424	1.3981	−0.1110	1.3077
	4.4	1.4696	1.6508	1.8114	−0.0598	1.3048	1.0456	1.2302	1.3770	−0.1142	1.3111
	4.6	1.4453	1.6152	1.7652	−0.0621	1.3064	1.0436	1.2192	1.3580	−0.1172	1.3144
	4.8	1.4233	1.5832	1.7239	−0.0642	1.3079	1.0417	1.2092	1.3408	−0.1200	1.3171
	5.0	1.4033	1.5544	1.6868	−0.0661	1.3093	1.0400	1.2000	1.3251	−0.1222	1.3200

and

$$\beta_2 = \frac{Q(0.875) - Q(0.625) - Q(0.375) + Q(0.125)}{Q(0.75) - Q(0.25)}.$$

For a selection of u values and parameter values, Table 1 shows the possible quantile values, Q_1, Q_2, Q_3, β_1, and β_2 of the Tr-PCJD. In Table 1 as κ increases, the quantiles (Q_1, Q_2, Q_3) gradually decrease, showing a downward trend. Similarly, β_1 shifts from slightly positive or near-zero values to increasingly negative values, while β_2 remains relatively stable with minimal variation. Comparing $\eta = 0.2$ and $\eta = 0.6$, higher η consistently results in lower quantile values, indicating that increasing η affects the distribution significantly.

Moments measures

Moments are essential statistical measures used in various scientific fields. The sth moment of a Tr-PCJD can be calculated using the following expression:

$$\mu'_s = \frac{\kappa\eta^2}{\eta+2}\int_0^\infty y^{s+\kappa-1}e^{-\eta y^\kappa}\left(\frac{(\eta y^{2\kappa}+1)}{\eta+2}\right)\left[1-\tau+2\tau e^{-\eta y^\kappa}\left(\frac{\eta y^\kappa(\eta y^\kappa+2)}{\eta+2}+1\right)\right] = I_1 + I_2 + I_3, \quad (8)$$

where,

$$I_1 = \frac{\kappa\eta^2}{\eta+2}\int_0^\infty y^{s+k-1}e^{-\eta y^\kappa}\left(\frac{(\eta y^{2\kappa}+1)}{\eta+2}\right)[1-\tau]\,dy,$$

$$I_2 = \frac{\kappa\eta^2}{\eta+2}\int_0^\infty y^{s+\kappa-1}e^{-\eta y^\kappa}\left(\frac{(\eta y^{2\kappa}+1)}{\eta+2}\right)\left[2\tau e^{-\eta y^\kappa}\left(\frac{\eta y^\kappa(\eta y^\kappa+2)}{\eta+2}\right)\right]dy,$$

and

$$I_3 = \frac{2\tau\kappa\eta^2}{\eta+2}\int_0^\infty y^{s+\kappa-1}e^{-2\eta y^\kappa}\left(\frac{(\eta y^{2\kappa}+1)}{\eta+2}\right)dy.$$

The integrals given in Eq. (8) can be obtained as below:

$$I_1 = \frac{\kappa\eta^3(1-\tau)}{(\eta+2)^2}\int_0^\infty y^{s+3\kappa-1}e^{-\eta y^\kappa}\,dy + \frac{\kappa\eta^2(1-\tau)}{(\eta+2)^2}\int_0^\infty y^{s+\kappa-1}e^{-\eta y^\kappa}\,dy$$
$$= \frac{\eta^{-(s/\kappa)}(1-\tau)}{(\eta+2)^2}\Gamma\left(\frac{s}{\kappa}+3\right) + \frac{\eta^{1-(s/\kappa)}(1-\tau)}{(\eta+2)^2}\Gamma\left(\frac{s}{\kappa}+1\right)$$

$$= \frac{(1-\tau)}{(\eta+2)^2\eta^{(s/\kappa)}}\left\{\Gamma\left(\frac{s}{\kappa}+3\right)+\eta\Gamma\left(\frac{s}{\kappa}+1\right)\right\},$$

$$I_2 = \frac{\kappa\eta^2}{\eta+2}\int_0^\infty y^{s+k-1}e^{-\eta y^\kappa}\left(\frac{(\eta y^{2\kappa}+1)}{\eta+2}\right)\left[2\tau e^{-\eta y^\kappa}\left(\frac{\eta y^\kappa(\eta y^\kappa+2)}{\eta+2}\right)\right]dy$$
$$= \frac{2\tau\kappa\eta^2}{(\eta+2)^3}\int_0^\infty y^{s+k-1}e^{-2\eta y^\kappa}(\eta y^{2\kappa}+1)(\eta y^\kappa(\eta y^\kappa+2))dy$$
$$= \frac{2\tau\kappa\eta^2}{(\eta+2)^3}\int_0^\infty y^{s+k-1}e^{-2\eta y^\kappa}(\eta^3y^{4\kappa}+\eta^2y^{2\kappa}+2\eta^2y^{3\kappa}+2\eta y^\kappa)dy,$$

then,

$$I_2 = \frac{2\tau\kappa\eta^2}{(\eta+2)^3}\int_0^\infty(\eta^3y^{s+5\kappa-1}+\eta^2y^{s+3\kappa-1}+2\eta^2y^{s+4\kappa-1}+2\eta y^{s+2\kappa-1})e^{-2\eta y^\kappa}dy$$
$$= \frac{2\tau\eta^2}{(2\eta)^{s/\kappa}(\eta+2)^3}\left[\frac{\eta^3}{(2\eta)^5}\Gamma\left(\frac{s}{\kappa}+5\right)+\frac{\eta^2}{(2\eta)^3}\Gamma\left(\frac{s}{\kappa}+3\right)+\frac{2\eta^2}{(2\eta)^4}\Gamma\left(\frac{s}{\kappa}+4\right)+\frac{2\eta}{(2\eta)^2}\Gamma\left(\frac{s}{\kappa}+2\right)\right]$$
$$= \frac{\tau}{(2\eta)^{s/\kappa}(\eta+2)^3}\left[\frac{1}{16}\Gamma\left(\frac{s}{\kappa}+5\right)+\frac{\eta}{4}\Gamma\left(\frac{s}{\kappa}+3\right)+\frac{1}{4}\Gamma\left(\frac{s}{\kappa}+4\right)+\eta\Gamma\left(\frac{s}{\kappa}+2\right)\right],$$

and

$$I_3 = \frac{2\tau\kappa\eta^2}{(\eta+2)^2}\int_0^\infty y^{s+\kappa-1}e^{-2\eta y^\kappa}\left(\eta y^{2\kappa}+1\right) = \frac{2\tau\kappa\eta^2}{(\eta+2)^2}\int_0^\infty \eta y^{s+3\kappa-1}e^{-2\eta y^\kappa}dy+\int_0^\infty y^{s+\kappa-1}e^{-2\eta y^\kappa}dy$$
$$= \frac{\tau}{(\eta+2)^2(2\eta)^{s/\kappa}}\left[\frac{1}{4}\Gamma\left(\frac{s}{\kappa}+3\right)+\eta\Gamma\left(\frac{s}{\kappa}+1\right)\right].$$

Hence the sth moment of Tr-PCJD takes the following form

$$\mu'_s = \frac{(1-\tau)}{(\eta+2)^2\eta^{(s/\kappa)}}\left\{\Gamma\left(\frac{s}{\kappa}+3\right)+\eta\Gamma\left(\frac{s}{\kappa}+1\right)\right\}+\frac{\tau}{(\eta+2)^2(2\eta)^{s/\kappa}}\left[\frac{1}{4}\Gamma\left(\frac{s}{\kappa}+3\right)+\eta\Gamma\left(\frac{s}{\kappa}+1\right)\right]$$
$$+\frac{\tau}{(2\eta)^{s/\kappa}(\eta+2)^3}\left[\frac{1}{16}\Gamma\left(\frac{s}{\kappa}+5\right)+\frac{\eta}{4}\Gamma\left(\frac{s}{\kappa}+3\right)+\frac{1}{4}\Gamma\left(\frac{s}{\kappa}+4\right)+\eta\Gamma\left(\frac{s}{\kappa}+2\right)\right],$$

where $\Gamma(.)$ is the gamma function (GF).

Furthermore, using moments around the origin, we may compute the sth central moment of Y based on the complete moments as follows:

$$\mu_n = E\left[(Y-E(Y))^n\right] = \sum_{k=0}^n(-1)^k\binom{n}{k}(E(Y))^k(E(Y))^{n-k}.$$

Next, we get skewness coefficient (λ_1), where $\lambda_1 = \mu_3/\mu_2^{1.5}$ and kurtosis coefficient (λ_2), where $\lambda_2 = \mu_4/\mu_2^2$. They play a crucial role in identifying the symmetry or asymmetry of the Tr-PCJD. Tables 2 and 3 present comprehensive numerical results for important statistical moments and parameters related to the Tr-PCJD model. The findings include the variance (σ^2), the standard deviation (σ), the skewness (λ_1), kurtosis (λ_2), and the coefficient of variation (CV). The first four moments are μ'_1, μ'_2, μ'_3, and μ'_4. The moments' values tend to drop as κ rises, indicating changes in the model's distribution. The tables also show how the dispersion and form characteristics vary from 0.2 to 0.6 for different values of τ. This highlights the sensitivity of the model to these important parameters and their influence on the results.

Similarly, using PDF in Eq. (6), the sth IM of the Tr-PCJD is ascertained as follows:

$$\mu'_s(c) = \frac{\kappa\eta^2}{\eta+2}\int_0^c y^{s+\kappa-1}e^{-\eta y^\kappa}\left(\frac{(\eta y^{2\kappa}+1)}{\eta+2}\right)\left[1-\tau+2\tau e^{-\eta y^\kappa}\left(\frac{\eta y^\kappa(\eta y^\kappa+2)}{\eta+2}+1\right)\right].$$

Using the above procedure discussed, the integrals J_1, J_2, and J_3 with upper limit c are given by:

$$J_1 = \frac{\kappa\eta^3(1-\tau)}{(\eta+2)^2}\int_0^c y^{s+3\kappa-1}e^{-\eta y^\kappa}dy+\frac{\kappa\eta^2(1-\tau)}{(\eta+2)^2}\int_0^c y^{s+k-1}e^{-\eta y^\kappa}dy$$
$$= \frac{(1-\tau)}{(\eta+2)^2\eta^{(s/\kappa)}}\left\{\gamma\left(\frac{s}{\kappa}+3,\eta c^\kappa\right)+\eta\gamma\left(\frac{s}{\kappa}+1,\eta c^\kappa\right)\right\},$$

$$J_2 = \frac{2\tau\kappa\eta^2}{(\eta+2)^3}\int_0^c(\eta^3y^{s+5\kappa-1}+\eta^2y^{s+3\kappa-1}+2\eta^2y^{s+4\kappa-1}+2\eta y^{s+2\kappa-1})e^{-2\eta y^\kappa}dy$$
$$= \frac{\tau}{(2\eta)^{s/\kappa}(\eta+2)^3}\left[\frac{1}{16}\gamma\left(\frac{s}{\kappa}+5,2\eta c^\kappa\right)+\frac{\eta}{4}\gamma\left(\frac{s}{\kappa}+3,2\eta c^\kappa\right)+\frac{1}{4}\gamma\left(\frac{s}{\kappa}+4,2\eta c^\kappa\right)+\eta\gamma\left(\frac{s}{\kappa}+2,2\eta c^\kappa\right)\right],$$

and

$$J_3 = \frac{2\tau\kappa\eta^2}{(\eta+2)^2}\int_0^c y^{s+\kappa-1}e^{-2\eta y^\kappa}\left(\eta y^{2\kappa}+1\right) = \frac{\tau}{(\eta+2)^2(2\eta)^{s/\kappa}}\left[\frac{1}{4}\gamma\left(\frac{s}{\kappa}+3,2\eta c^\kappa\right)+\eta\Gamma\left(\frac{s}{\kappa}+1,2\eta c^\kappa\right)\right],$$

Table 2
Numerical outcomes for the first four moments, σ^2, σ, λ_1, λ_2 and CV for the Tr-PCJD when $\tau = 0.2$.

τ	κ	μ_1'	μ_2'	μ_3'	μ_4'	σ^2	σ	λ_1	λ_2	CV
0.5	2.4	2.6257	7.5202	23.0162	74.5102	0.6260	0.7912	−0.0337	3.2173	0.3013
	2.6	2.4293	6.3664	17.6863	51.6212	0.4649	0.6818	−0.1219	3.2668	0.2807
	2.8	2.2737	5.5265	14.1463	37.8343	0.3570	0.5975	−0.2003	3.3341	0.2628
	3.0	2.1475	4.8936	11.6787	28.9885	0.2817	0.5308	−0.2708	3.4131	0.2472
	3.2	2.0434	4.4029	9.8899	23.0162	0.2274	0.4769	−0.3345	3.5000	0.2334
	3.4	1.9561	4.0134	8.5506	18.8120	0.1870	0.4325	−0.3926	3.5920	0.2211
	3.6	1.8819	3.6980	7.5202	15.7478	0.1563	0.3954	−0.4458	3.6871	0.2101
	3.8	1.8182	3.4382	6.7091	13.4481	0.1324	0.3639	−0.4947	3.7838	0.2001
	4.0	1.7628	3.2212	6.0581	11.6787	0.1135	0.3370	−0.5400	3.8811	0.1911
	4.2	1.7144	3.0374	5.5265	10.2880	0.0984	0.3136	−0.5819	3.9782	0.1829
	4.4	1.6716	2.8801	5.0862	9.1744	0.0860	0.2932	−0.6210	4.0745	0.1754
	4.6	1.6335	2.7442	4.7166	8.2682	0.0758	0.2753	−0.6574	4.1696	0.1685
	4.8	1.5995	2.6257	4.4029	7.5202	0.0673	0.2594	−0.6916	4.2633	0.1622
	5.0	1.5689	2.5215	4.1339	6.8949	0.0601	0.2452	−0.7236	4.3553	0.1563
0.8	2.4	2.4880	6.7407	19.4697	59.3578	0.5507	0.7421	−0.1007	3.2941	0.2983
	2.6	2.3116	5.7565	15.1654	41.8977	0.4131	0.6427	−0.1910	3.3503	0.2780
	2.8	2.1712	5.0342	12.2707	31.1987	0.3200	0.5657	−0.2712	3.4246	0.2605
	3.0	2.0571	4.4862	10.2314	24.2327	0.2544	0.5044	−0.3431	3.5108	0.2452
	3.2	1.9627	4.0589	8.7394	19.4697	0.2067	0.4546	−0.4081	3.6049	0.2316
	3.4	1.8833	3.7179	7.6132	16.0795	0.1710	0.4135	−0.4673	3.7037	0.2196
	3.6	1.8158	3.4406	6.7407	13.5844	0.1437	0.3790	−0.5214	3.8054	0.2087
	3.8	1.7576	3.2114	6.0497	11.6957	0.1223	0.3497	−0.5712	3.9084	0.1990
	4.0	1.7070	3.0191	5.4919	10.2314	0.1053	0.3245	−0.6171	4.0116	0.1901
	4.2	1.6626	2.8558	5.0342	9.0725	0.0916	0.3026	−0.6597	4.1144	0.1820
	4.4	1.6234	2.7156	4.6533	8.1388	0.0803	0.2834	−0.6994	4.2161	0.1746
	4.6	1.5884	2.5941	4.3323	7.3747	0.0710	0.2665	−0.7363	4.3164	0.1678
	4.8	1.5572	2.4880	4.0589	6.7407	0.0632	0.2515	−0.7709	4.4149	0.1615
	5.0	1.5290	2.3945	3.8236	6.2084	0.0567	0.2380	−0.8034	4.5115	0.1557

where $\gamma(.,.)$ is the lower incomplete GF. Hence the sth incomplete moment of the Tr-PCJD is as below:

$$\mu'_s(c) = \frac{(1-\tau)}{(\eta+2)^2\eta^{(s/\kappa)}}\left\{\gamma\left(\frac{s}{\kappa}+3, 2\eta c^{\kappa}\right)+\eta\gamma\left(\frac{s}{\kappa}+1, 2\eta c^{\kappa}\right)\right\}$$
$$+\frac{\tau}{(\eta+2)^2(2\eta)^{s/\kappa}}\left[\frac{1}{4}\gamma\left(\frac{s}{\kappa}+3, 2\eta c^{\kappa}\right)+\eta\gamma\left(\frac{s}{\kappa}+1, 2\eta c^{\kappa}\right)\right]$$
$$+\frac{\tau}{(2\eta)^{s/\kappa}(\eta+2)^3}\left[\frac{1}{16}\gamma\left(\frac{s}{\kappa}+5, 2\eta c^{\kappa}\right)+\frac{\eta}{4}\gamma\left(\frac{s}{\kappa}+3, 2\eta c^{\kappa}\right)+\frac{1}{4}\gamma\left(\frac{s}{\kappa}+4, 2\eta c^{\kappa}\right)+\eta\gamma\left(\frac{s}{\kappa}+2, 2\eta c^{\kappa}\right)\right].$$

Information measures

Information theory and thermodynamics both depend on the concept of entropy, which is a measure of disorder or uncertainty. It counts the number of configurations or states that a system can have. Greater chaos is indicated by higher entropy, whereas more order is suggested by lower entropy. The degree of order or structure within a system is represented by the relatively new term of extropy. Since it quantifies the degree of order or predictability, it is frequently thought of as the antithesis of entropy. Extropy is related to order, coherence, and pattern, whereas entropy is connected to chaos and unpredictability. Essentially, entropy and extropy offer complementary viewpoints on a system's state and dynamics, revealing aspects of its order and chaos, respectively.

Let Y be non-negative random variable with a PDF that represents the lifetime of a system or component. Based on Lad and Sanfilippo [26], the differential extropy (Exy) of Y can be defined as follows:

$$\Delta = \frac{-1}{2}\int_0^{\infty} f^2(y)dy. \tag{9}$$

The Tr-PCJD's Exy is displayed by obtaining it as shown below.

$$f^2(y) = \frac{\kappa^2\eta^4(1-\tau)^2}{(\eta+2)^4}y^{2(\kappa-1)}e^{-2\eta y^{\kappa}}\left(\eta y^{2\kappa}+1\right)^2\left[1+\frac{2\tau e^{-\eta y^{\kappa}}}{1-\tau}\left(\frac{\eta y^{\kappa}(\eta y^{\kappa}+2)}{\eta+2}+1\right)\right]^2. \tag{10}$$

The last term in Eq. (10) can be rewritten as follows

$$\left[1+\frac{2\tau e^{-\eta y^{\kappa}}}{1-\tau}\left(\frac{\eta y^{\kappa}(\eta y^{\kappa}+2)}{\eta+2}+1\right)\right]^2 = 1+\frac{4\tau e^{-\eta y^{\kappa}}}{1-\tau}\left(\frac{\eta y^{\kappa}(\eta y^{\kappa}+2)}{\eta+2}+1\right)$$
$$+\frac{4\tau^2 e^{-2\eta y^{\kappa}}}{(1-\tau)^2}\left(\frac{\eta y^{\kappa}(\eta y^{\kappa}+2)}{\eta+2}+1\right)^2 = A_1 + A_2, \tag{11}$$

Table 3
Numerical outcomes for the first four moments, σ^2, σ, λ_1, λ_2 and CV for the Tr-PCJD when $\tau = 0.6$.

τ	κ	μ_1'	μ_2'	μ_3'	μ_4'	σ^2	σ	λ_1	λ_2	CV
0.5	2.4	1.5355	2.6688	5.0481	10.2009	0.3111	0.5577	−0.0295	2.8198	0.3632
	2.6	1.4780	2.4362	4.3300	8.1638	0.2516	0.5016	−0.1156	2.8386	0.3394
	2.8	1.4313	2.2567	3.8074	6.7743	0.2080	0.4561	−0.1916	2.8751	0.3186
	3.0	1.3927	2.1146	3.4135	5.7825	0.1750	0.4183	−0.2594	2.9235	0.3004
	3.2	1.3602	1.9996	3.1080	5.0481	0.1495	0.3866	−0.3203	2.9799	0.2842
	3.4	1.3325	1.9049	2.8654	4.4877	0.1292	0.3595	−0.3755	3.0416	0.2698
	3.6	1.3087	1.8257	2.6688	4.0492	0.1129	0.3361	−0.4258	3.1067	0.2568
	3.8	1.2880	1.7586	2.5068	3.6987	0.0996	0.3156	−0.4718	3.1737	0.2450
	4.0	1.2698	1.7010	2.3714	3.4135	0.0886	0.2976	−0.5141	3.2418	0.2343
	4.2	1.2538	1.6512	2.2567	3.1776	0.0793	0.2816	−0.5532	3.3101	0.2246
	4.4	1.2395	1.6077	2.1585	2.9800	0.0714	0.2672	−0.5895	3.3782	0.2156
	4.6	1.2267	1.5694	2.0736	2.8124	0.0647	0.2543	−0.6232	3.4457	0.2073
	4.8	1.2152	1.5355	1.9996	2.6688	0.0589	0.2427	−0.6547	3.5123	0.1997
	5.0	1.2047	1.5052	1.9346	2.5446	0.0539	0.2321	−0.6841	3.5779	0.1926
0.8	2.4	1.4384	2.3448	4.1592	7.8794	0.2757	0.5251	−0.0472	2.8226	0.3651
	2.6	1.3915	2.1616	3.6209	6.4325	0.2254	0.4748	−0.1332	2.8367	0.3412
	2.8	1.3533	2.0194	3.2247	5.4293	0.1881	0.4337	−0.2090	2.8696	0.3205
	3.0	1.3216	1.9061	2.9231	4.7032	0.1595	0.3994	−0.2765	2.9151	0.3022
	3.2	1.2949	1.8140	2.6872	4.1592	0.1372	0.3704	−0.3371	2.9690	0.2860
	3.4	1.2722	1.7379	2.4986	3.7398	0.1194	0.3455	−0.3918	3.0284	0.2715
	3.6	1.2527	1.6741	2.3448	3.4086	0.1049	0.3238	−0.4416	3.0915	0.2585
	3.8	1.2357	1.6198	2.2174	3.1418	0.0930	0.3049	−0.4872	3.1567	0.2467
	4.0	1.2207	1.5732	2.1104	2.9231	0.0830	0.2881	−0.5291	3.2230	0.2360
	4.2	1.2075	1.5327	2.0194	2.7412	0.0746	0.2731	−0.5678	3.2896	0.2262
	4.4	1.1958	1.4973	1.9412	2.5879	0.0675	0.2597	−0.6036	3.3562	0.2172
	4.6	1.1852	1.4661	1.8734	2.4572	0.0613	0.2476	−0.6369	3.4221	0.2089
	4.8	1.1758	1.4384	1.8140	2.3448	0.0560	0.2366	−0.6679	3.4873	0.2012
	5.0	1.1672	1.4137	1.7618	2.2471	0.0513	0.2266	−0.6970	3.5513	0.1941

where,

$$A_1 = 1 + \frac{4\tau\eta^2 y^{2\kappa} e^{-\eta y^\kappa}}{(1-\tau)(\eta+2)} + \frac{8\tau\eta y^\kappa e^{-\eta y^\kappa}}{(1-\tau)(\eta+2)} + \frac{4\tau e^{-\eta y^\kappa}}{1-\tau},$$

and

$$A_2 = \frac{4\tau^2\eta^4 y^{4\kappa} e^{-2\eta y^\kappa}}{(\eta+2)^2(1-\tau)^2} + \frac{16\tau^2\eta^3 y^{3\kappa} e^{-2\eta y^\kappa}}{(1-\tau)^2(\eta+2)^2} + \frac{16\tau^2\eta^2 y^{2\kappa} e^{-2\eta y^\kappa}}{(\eta+2)^2(1-\tau)^2} + \frac{4\tau^2 e^{-2\eta y^\kappa}}{(1-\tau)^2} + \frac{8\tau^2\eta^2 y^{2\kappa} e^{-2\eta y^\kappa}}{(1-\tau)^2(\eta+2)} + \frac{16\tau^2\eta y^\kappa e^{-2\eta y^\kappa}}{(1-\tau)^2(\eta+2)}.$$

Inserting Eq. (11) in Eq. (10) gives

$$f^2(y) = \frac{\kappa^2\eta^4(1-\tau)^2}{(\eta+2)^4} y^{2\kappa-2} e^{-2\eta y^\kappa} \left(\eta^2 y^{4\kappa} + 2\eta y^{2\kappa} + 1\right)(A_1 + A_2). \tag{12}$$

Inserting Eq. (12) in Eq. (9)

$$\begin{aligned} \Delta = \frac{-\kappa^2\eta^4(1-\tau)^2}{2(\eta+2)^4} \int_0^\infty y^{2\kappa-2} e^{-2\eta y^\kappa} \left(\eta^2 y^{4\kappa} + 2\eta y^{2\kappa} + 1\right)(A_1 + A_2) dy \\ = \int_0^\infty (B_1 + B_2) dy = B_1^* + B_2^*, \end{aligned} \tag{13}$$

where

$$B_1 = \frac{-\kappa^2\eta^4(1-\tau)^2}{2(\eta+2)^4} \left[y^{2\kappa-2} e^{-2\eta y^\kappa} \left(\eta^2 y^{4\kappa} + 2\eta y^{2\kappa} + 1\right) A_1 \right],$$

$$B_2 = \frac{-\kappa^2\eta^4(1-\tau)^2}{2(\eta+2)^4} \left[y^{2\kappa-2} e^{-2\eta y^\kappa} \left(\eta^2 y^{4\kappa} + 2\eta y^{2\kappa} + 1\right) A_2 \right].$$

$$\begin{aligned} B_1^* = \int_0^\infty B_1 dy = \frac{-\kappa^2\eta^4(1-\tau)^2}{2(\eta+2)^4} \int_0^\infty y^{2\kappa-2} e^{-2\eta y^\kappa} \left(\eta^2 y^{4\kappa} + 2\eta y^{2\kappa} + 1\right) \\ \times \left[1 + \frac{4\tau\eta^2 y^{2\kappa} e^{-\eta y^\kappa}}{(1-\tau)(\eta+2)} + \frac{8\tau\eta y^\kappa e^{-\eta y^\kappa}}{(1-\tau)(\eta+2)} + \frac{4\tau e^{-\eta y^\kappa}}{1-\tau} \right] dy \\ = B_{11} + B_{12} + B_{13} + B_{14} \end{aligned}$$

$$
\begin{aligned}
B_{11} &= \frac{-\kappa^2\eta^4(1-\tau)^2}{2(\eta+2)^4}\int_0^\infty (\eta^2 y^{6\kappa-2}e^{-2\eta y^\kappa} + 2\eta y^{4\kappa-2}e^{-2\eta y^\kappa} + y^{2\kappa-2}e^{-2\eta y^\kappa})dy \\
&= \frac{-\kappa(1-\tau)^2}{8(\eta+2)^4}\left[\frac{1}{16}\Gamma\left(6-\frac{1}{\kappa}\right) + \frac{\eta}{4}\Gamma\left(4-\frac{1}{\kappa}\right) + \eta^2\Gamma\left(2-\frac{1}{\kappa}\right)\right]
\end{aligned}
$$

$$
\begin{aligned}
B_{12} &= \frac{-2\kappa^2\eta^6\tau(1-\tau)}{(\eta+2)^5}\int_0^\infty (\eta^2 y^{8\kappa-2}e^{-3\eta y^\kappa} + 2\eta y^{6\kappa-2}e^{-3\eta y^\kappa} + y^{2\kappa-2}e^{-3\eta y^\kappa})\ dy \\
&= \frac{-2\kappa(3\eta)^{(1/\kappa)}(1-\tau)\tau}{(3)^2(\eta+2)^5}\left[\frac{1}{(3)^6}\Gamma\left(8-\frac{1}{\kappa}\right) + \frac{2\eta}{(3)^4}\Gamma\left(6-\frac{1}{\kappa}\right) + \eta^4\Gamma\left(2-\frac{1}{\kappa}\right)\right],
\end{aligned}
$$

$$
\begin{aligned}
B_{13} &= \frac{-4\kappa^2(1-\tau)\eta^5\tau}{(\eta+2)^5}\int_0^\infty (\eta^2 y^{7\kappa-2}e^{-3\eta y^\kappa} + 2\eta y^{5\kappa-2}e^{-3\eta y^\kappa} + y^{3\kappa-2}e^{-3\eta y^\kappa})dy \\
&= \frac{-4\kappa(1-\tau)(3\eta)^{(1/\kappa)}\tau}{3^3(\eta+2)^5}\left[\frac{1}{3^4}\Gamma\left(7-\frac{1}{\kappa}\right) + \frac{2\eta}{3^2}\Gamma\left(5-\frac{1}{\kappa}\right) + \eta^2\Gamma\left(3-\frac{1}{\kappa}\right)\right],
\end{aligned}
$$

$$
\begin{aligned}
B_{14} &= \frac{-2\tau\kappa^2(1-\tau)\eta^4}{(\eta+2)^4}\int_0^\infty (\eta^2 y^{6\kappa-2}e^{-3\eta y^\kappa} + 2\eta y^{4\kappa-2}e^{-3\eta y^\kappa} + y^{2\kappa-2}e^{-3\eta y^\kappa})dy \\
&= \frac{-2\tau\kappa^2(1-\tau)}{9(\eta+2)^4}\left[\frac{1}{3^4}\Gamma\left(6-\frac{1}{\kappa}\right) + \frac{2}{3^2\eta}\Gamma\left(4-\frac{1}{\kappa}\right) + \eta^2\Gamma\left(2-\frac{1}{\kappa}\right)\right],
\end{aligned}
$$

$$
\begin{aligned}
B_1^* = &\frac{-\kappa(1-\tau)^2}{(\eta+2)^4}\left[\frac{1}{2^7}\Gamma\left(6-\frac{1}{\kappa}\right) + \frac{\eta}{2^4}\Gamma\left(4-\frac{1}{\kappa}\right) + \frac{\eta^2}{2^3}\Gamma\left(2-\frac{1}{\kappa}\right)\right] \\
&\frac{-2\kappa(3\eta)^{(1/\kappa)}(1-\tau)\tau}{(3)^2(\eta+2)^5}\left[\frac{1}{(3)^6}\Gamma\left(8-\frac{1}{\kappa}\right) + \frac{2\eta}{(3)^4}\Gamma\left(6-\frac{1}{\kappa}\right) + \eta^4\Gamma\left(2-\frac{1}{\kappa}\right)\right] \\
&\frac{-4\kappa(1-\tau)(3\eta)^{(1/\kappa)}\tau}{3^3(\eta+2)^5}\left[\frac{1}{3^4}\Gamma\left(7-\frac{1}{\kappa}\right) + \frac{2\eta}{3^2}\Gamma\left(5-\frac{1}{\kappa}\right) + \eta^2\Gamma\left(3-\frac{1}{\kappa}\right)\right] \\
&\frac{-2\tau\kappa^2(1-\tau)}{9(\eta+2)^4}\left[\frac{1}{3^4}\Gamma\left(6-\frac{1}{\kappa}\right) + \frac{2}{3^2\eta}\Gamma\left(4-\frac{1}{\kappa}\right) + \eta^2\Gamma\left(2-\frac{1}{\kappa}\right)\right].
\end{aligned} \tag{14}
$$

$$
\begin{aligned}
B_2^* = &\frac{-\kappa^2\eta^4(1-\tau)^2}{2(\eta+2)^4}\int_0^\infty y^{2(\kappa-1)}e^{-2\eta y^\kappa}\left(\eta^2 y^{2\kappa} + 2\eta y^{2\kappa} + 1\right) \\
&\times\left[\frac{4\tau^2\eta^4 y^{4\kappa}e^{-2\eta y^\kappa}}{(\eta+2)^2(1-\tau)^2} + \frac{16\tau^2\eta^3 y^{3\kappa}e^{-2\eta y^\kappa}}{(1-\tau)^2(\eta+2)^2} + \frac{16\tau^2\eta^2 y^{2\kappa}e^{-2\eta y^\kappa}}{(\eta+2)^2(1-\tau)^2}\right. \\
&\left.+\frac{4\tau^2 e^{-2\eta y^\kappa}}{(1-\tau)^2} + \frac{8\tau^2\eta^2 y^{2\kappa}e^{-2\eta y^\kappa}}{(1-\tau)^2(\eta+2)} + \frac{16\tau^2\eta y^\kappa e^{-2\eta y^\kappa}}{(1-\tau)^2(\eta+2)}\right]dy \\
&= B_{21} + B_{22} + B_{23} + B_{31} + B_{32} + B_{33},
\end{aligned}
$$

$$
\begin{aligned}
B_{21} &= \frac{-\kappa^2\eta^4(1-\tau)^2}{2(\eta+2)^4}\int_0^\infty y^{2\kappa-2}e^{-2\eta y^\kappa}\left(\eta^2 y^{4\kappa} + 2\eta y^{2\kappa} + 1\right)\left[\frac{4\tau^2\eta^4 y^{4\kappa}e^{-2\eta y^\kappa}}{(\eta+2)^2(1-\tau)^2}\right]dy \\
&= \frac{-2\kappa^2\eta^8\tau^2}{(\eta+2)^6}\int_0^\infty\left(\eta^2 y^{10\kappa-2}e^{-4\eta y^\kappa} + 2\eta y^{8\kappa-2}e^{-4\eta y^\kappa} + y^{6\kappa-2}e^{-4\eta y^\kappa}\right) \\
&= \frac{-\tau^2\kappa(4\eta)^{1/\kappa}}{(2)^{11}(\eta+2)^6}\left[\frac{1}{(4)^4}\Gamma\left(10-\frac{1}{\kappa}\right) + \frac{1}{8\eta}\Gamma\left(8-\frac{1}{\kappa}\right) + \eta^2\Gamma\left(6-\frac{1}{\kappa}\right)\right],
\end{aligned}
$$

$$
\begin{aligned}
B_{22} &= \frac{-\kappa^2\eta^4(1-\tau)^2}{2(\eta+2)^4}\int_0^\infty y^{2\kappa-2}e^{-2\eta y^\kappa}\left(\eta^2 y^{4\kappa} + 2\eta y^{2\kappa} + 1\right)\left[\frac{16\tau^2\eta^3 y^{3\kappa}e^{-2\eta y^\kappa}}{(1-\tau)^2(\eta+2)^2}\right]dy \\
&= \frac{-8\tau^2\kappa^2\eta^7}{(\eta+2)^6}\int_0^\infty e^{-4\eta y^\kappa}\left(\eta^2 y^{9\kappa-2} + 2\eta y^{7\kappa-2} + y^{5\kappa-2}\right)dy \\
&= \frac{-\kappa\tau^2(4\eta)^{1/\kappa}}{2^7(\eta+2)^4}\left[\frac{1}{4^4}\Gamma\left(9-\frac{1}{\kappa}\right) + \frac{1}{8\eta}\Gamma\left(7-\frac{1}{\kappa}\right) + \eta^2\Gamma\left(5-\frac{1}{\kappa}\right)\right],
\end{aligned}
$$

$$
\begin{aligned}
B_{23} &= \frac{-\kappa^2\eta^4(1-\tau)^2}{2(\eta+2)^4}\int_0^\infty y^{2\kappa-2}e^{-2\eta y^\kappa}\left(\eta^2 y^{4\kappa} + 2\eta y^{2\kappa} + 1\right)\left[\frac{16\tau^2\eta^2 y^{2\kappa}e^{-2\eta y^\kappa}}{(\eta+2)^2(1-\tau)^2}\right]dy \\
&= \frac{-8\tau^2\kappa^2\eta^6}{(\eta+2)^6}\int_0^\infty e^{-4\eta y^\kappa}\left(\eta^2 y^{8\kappa-2} + 2\eta y^{6\kappa-2} + y^{4\kappa-2}\right)dy
\end{aligned}
$$

$$= \frac{-\tau^2\kappa(4\eta)^{1/\kappa}\eta^6}{2^5(\eta+2)^6}\left[\frac{1}{4^4}\Gamma\left(8-\frac{1}{\kappa}\right)+\frac{1}{8\eta}\Gamma\left(6-\frac{1}{\kappa}\right)+\eta^2\Gamma\left(4-\frac{1}{\kappa}\right)\right],$$

$$\begin{aligned}B_{31} &= \frac{-\kappa^2\eta^4(1-\tau)^2}{2(\eta+2)^4}\int_0^\infty y^{2\kappa-2}e^{-2\eta y^\kappa}\left(\eta^2y^{4\kappa}+2\eta y^{2\kappa}+1\right)\left(\frac{4\tau^2e^{-2\eta y^\kappa}}{(1-\tau)^2}\right)dy\\ &= \frac{-2\tau^2\kappa^2\eta^4}{(\eta+2)^4}\int_0^\infty e^{-4\eta y^\kappa}\left(\eta^2y^{6\kappa-2}+2\eta y^{4\kappa-2}+y^{2\kappa-2}\right)dy\\ &= \frac{-\tau^2(4\eta)^{1/\kappa}\kappa}{8(\eta+2)^4}\left[\frac{1}{4^4}\Gamma\left(6-\frac{1}{\kappa}\right)+\frac{\eta}{4^2}\Gamma\left(4-\frac{1}{\kappa}\right)+\Gamma\left(2-\frac{1}{\kappa}\right)\right],\end{aligned}$$

$$\begin{aligned}B_{32} &= \frac{-\kappa^2\eta^4(1-\tau)^2}{2(\eta+2)^4}\int_0^\infty y^{2\kappa-2}e^{-2\eta y^\kappa}\left(\eta^2y^{4\kappa}+2\eta y^{2\kappa}+1\right)\left(\frac{8\tau^2\eta^2y^{2\kappa}e^{-2\eta y^\kappa}}{(1-\tau)^2(\eta+2)}\right)dy\\ &= \frac{-4\tau^2\eta^6\kappa^2}{(\eta+2)^5}\int_0^\infty e^{-4\eta y^\kappa}\left(\eta^2y^{8\kappa-2}+2\eta y^{6\kappa-2}+y^{4\kappa-2}\right)dy\\ &= \frac{-4\tau^2(4\eta)^{1/\kappa}\kappa}{(\eta+2)^5}\left[\frac{1}{8}\Gamma\left(8-\frac{1}{\kappa}\right)+\frac{1}{4\eta}\Gamma\left(6-\frac{1}{\kappa}\right)+2\Gamma\left(4-\frac{1}{\kappa}\right)\right],\end{aligned}$$

$$\begin{aligned}B_{33} &= \frac{-\kappa^2\eta^4(1-\tau)^2}{2(\eta+2)^4}\int_0^\infty y^{2\kappa-2}e^{-2\eta y^\kappa}\left(\eta^2y^{4\kappa}+2\eta y^{2\kappa}+1\right)\left(\frac{16\tau^2\eta y^{\kappa}e^{-2\eta y^\kappa}}{(1-\tau)^2(\eta+2)}\right)dy\\ &= \frac{-8\tau^2\kappa^2\eta^5}{(\eta+2)^5}\int_0^\infty e^{-4\eta y^\kappa}\left(\eta^2y^{7\kappa-2}+2\eta y^{5\kappa-2}+y^{3\kappa-2}\right)dy\\ &= \frac{-\tau^2(2\eta)^{1/\kappa}\kappa}{(\eta+2)^5}\left[\frac{1}{16}\Gamma\left(7-\frac{1}{\kappa}\right)+\frac{1}{4\eta}\Gamma\left(5-\frac{1}{\kappa}\right)+\eta^2\Gamma\left(3-\frac{1}{\kappa}\right)\right],\end{aligned}$$

$$\begin{aligned}B_2^* = &\frac{-\tau^2\kappa(4\eta)^{1/\kappa}}{(2)^{11}(\eta+2)^6}\left[\frac{1}{4^4}\Gamma\left(10-\frac{1}{\kappa}\right)+\frac{1}{8\eta}\Gamma\left(8-\frac{1}{\kappa}\right)+\eta^2\Gamma\left(6-\frac{1}{\kappa}\right)\right]\\ &\frac{-\kappa\tau^2(4\eta)^{1/\kappa}}{2^7(\eta+2)^4}\left[\frac{1}{4^4}\Gamma\left(9-\frac{1}{\kappa}\right)+\frac{1}{8\eta}\Gamma\left(7-\frac{1}{\kappa}\right)+\eta^2\Gamma\left(5-\frac{1}{\kappa}\right)\right]\\ &\frac{-\tau^2\kappa(4\eta)^{1/\kappa}\eta^6}{2^5(\eta+2)^6}\left[\frac{1}{4^4}\Gamma\left(8-\frac{1}{\kappa}\right)+\frac{1}{8\eta}\Gamma\left(6-\frac{1}{\kappa}\right)+\eta^2\Gamma\left(4-\frac{1}{\kappa}\right)\right]\\ &\frac{-\tau^2(4\eta)^{1/\kappa}\kappa}{8(\eta+2)^4}\left[\frac{1}{4^4}\Gamma\left(6-\frac{1}{\kappa}\right)+\frac{\eta}{4^2}\Gamma\left(4-\frac{1}{\kappa}\right)+\Gamma\left(2-\frac{1}{\kappa}\right)\right]\\ &\frac{-4\tau^2(4\eta)^{1/\kappa}\kappa}{(\eta+2)^5}\left[\frac{1}{8}\Gamma\left(8-\frac{1}{\kappa}\right)+\frac{1}{4\eta}\Gamma\left(6-\frac{1}{\kappa}\right)+2\Gamma\left(4-\frac{1}{\kappa}\right)\right]\\ &\frac{-\tau^2(2\eta)^{1/\kappa}\kappa}{(\eta+2)^5}\left[\frac{1}{16}\Gamma\left(7-\frac{1}{\kappa}\right)+\frac{1}{4\eta}\Gamma\left(5-\frac{1}{\kappa}\right)+\eta^2\Gamma\left(3-\frac{1}{\kappa}\right)\right].\end{aligned} \tag{15}$$

Using Eqs. (14) and (15) in Eq. (13), the Exy measure is determined.

Estimation methods

In this section, we employ eight different estimation methods to determine the parameters η, κ and τ of Tr-PCJD. These estimates are MLE, ADE, CME, LSE, RADE, WLSE, ADLTSE, and PE. Also, a numerical study to examine the behavior of different estimates is given.

Maximum likelihood method

The MLE [27,28] is based on maximizing the log-likelihood function to estimate the parameters η, κ, and τ. Suppose that $y_1, y_2, \ldots, y_n$ is a random sample of size n from Tr-PCJD. Based on Eq. (6), the log-likelihood function can be expressed as follows:

$$\begin{aligned}l(\eta,\kappa,\tau) &= n\log(\kappa)+2n\log(\eta)-n\log(\eta+2)+(\kappa-1)\sum_{i=1}^n\log(y_i)-\eta\sum_{i=1}^n y_i^\kappa\\ &+\sum_{i=1}^n\log\left(\eta y_i^{2\kappa}+1\right)+\sum_{i=1}^n\log\left[1-\tau+2\tau e^{-\eta y_i^\kappa}\left(\frac{\eta y_i^\kappa(\eta y_i^\kappa+2)}{\eta+2}+1\right)\right].\end{aligned}$$

The MLEs $\hat{\eta}$, $\hat{\kappa}$, and $\hat{\tau}$ of η, κ, and τ, respectively, are obtained by solving the following nonlinear equations:

$$\frac{\partial l(\eta,\kappa,\tau)}{\partial\eta} = \frac{2n}{\eta}-\frac{n}{\eta+2}-\sum_{i=1}^n y_i^\kappa+\sum_{i=1}^n\frac{y_i^{2\kappa}}{\eta y_i^{2\kappa}+1}$$

$$+\sum_{i=1}^{n}\frac{-2\tau y_i^{\kappa}e^{-\eta y_i^{\kappa}}\left(\frac{\eta y_i^{\kappa}(\eta y_i^{\kappa}+2)}{\eta+2}+1\right)+2\tau e^{-\eta y_i^{\kappa}}\left(\frac{\eta y_i^{\kappa}(\eta+4)+4y_i^{\kappa}}{(\eta+2)^2}\right)}{1-\tau+2\tau e^{-\eta y_i^{\kappa}}\left(\frac{\eta y_i^{\kappa}(\eta y_i^{\kappa}+2)}{\eta+2}+1\right)}=0,$$

$$\frac{\partial l(\eta,\kappa,\tau)}{\partial\kappa}=\frac{n}{\kappa}+\sum_{i=1}^{n}\log(y_i)-\eta\sum_{i=1}^{n}y_i^{\kappa}\log(y_i)+\sum_{i=1}^{n}\frac{2\eta y_i^{2\kappa}\log(y_i)}{\eta y_i^{2\kappa}+1}$$
$$+\sum_{i=1}^{n}\frac{2\tau\left[-\eta y_i^{\kappa}\log(y_i)e^{-\eta y_i^{\kappa}}\left(\frac{\eta y_i^{\kappa}(\eta y_i^{\kappa}+2)}{\eta+2}+1\right)+e^{-\eta y_i^{\kappa}}\left(\frac{\eta y_i^{\kappa}\log(y_i)(\eta y_i^{\kappa}+2)+\eta^2y_i^{2\kappa}\log(y_i)}{\eta+2}\right)\right]}{1-\tau+2\tau e^{-\eta y_i^{\kappa}}\left(\frac{\eta y_i^{\kappa}(\eta y_i^{\kappa}+2)}{\eta+2}+1\right)}=0,$$

and,

$$\frac{\partial l(\eta,\kappa,\tau)}{\partial\tau}=\sum_{i=1}^{n}\frac{-1+2e^{-\eta y_i^{\kappa}}\left(\frac{\eta y_i^{\kappa}(\eta y_i^{\kappa}+2)}{\eta+2}+1\right)}{1-\tau+2\tau e^{-\eta y_i^{\kappa}}\left(\frac{\eta y_i^{\kappa}(\eta y_i^{\kappa}+2)}{\eta+2}+1\right)}=0.$$

Since an exact solution to these nonlinear equations is generally intractable, numerical methods and statistical software can be employed to obtain approximate solutions.

Anderson–Darling method

Suppose that $y_1, y_2, \dots, y_n$ be a random sample of size n from the Tr-PCJD and let $y_{(1)}, y_{(2)}, \dots, y_{(n)}$ represent the corresponding ordered samples. To estimate η, κ, and τ, the ADE (see [29]), involves minimizing the function:

$$A(\eta,\kappa,\tau)=-n-\frac{1}{n}\sum_{i=1}^{n}(2i-1)\left[\log F(y_{(i)})+\log(1-F(y_{(n-i+1)}))\right],$$

where $F(y_{(i)})$ is the CDF of the distribution. The partial derivatives of $A(\eta,\kappa,\tau)$ with respect to η, κ, and τ are given by:

$$\frac{\partial A(\eta,\kappa,\tau)}{\partial\eta}=-\frac{1}{n}\sum_{i=1}^{n}(2i-1)\left[\frac{F_{\eta_i}}{F_i}-\frac{F_{\eta_{n-i+1}}}{1-F_{n-i+1}}\right],$$

$$\frac{\partial A(\eta,\kappa,\tau)}{\partial\kappa}=-\frac{1}{n}\sum_{i=1}^{n}(2i-1)\left[\frac{F_{\kappa_i}}{F_i}-\frac{F_{\kappa_{n-i+1}}}{1-F_{n-i+1}}\right],$$

$$\frac{\partial A(\eta,\kappa,\tau)}{\partial\tau}=-\frac{1}{n}\sum_{i=1}^{n}(2i-1)\left[\frac{F_{\tau_i}}{F_i}-\frac{F_{\tau_{n-i+1}}}{1-F_{n-i+1}}\right],$$

where the quantities F_{η_i}, F_{κ_i}, and F_{τ_i} are the partial derivatives of the CDF with respect to η, κ, and τ, respectively, also $F_i = F(y_{(i)})$. The partial derivatives F_{η_i}, F_{κ_i}, and F_{τ_i} are obtained, respectively, as follows:

$$F_{\eta_i}=\frac{\partial F(y_{(i)})}{\partial\eta}=e^{-\eta y_{(i)}^{\kappa}}\left(1-\tau+2\tau e^{-\eta y_{(i)}^{\kappa}}\left(\frac{\eta y_{(i)}^{\kappa}(\eta y_{(i)}^{\kappa}+2)}{\eta+2}+1\right)\right)$$
$$\times\left[y_{(i)}^{\kappa}\left(\frac{\eta y_{(i)}^{\kappa}(\eta y_{(i)}^{\kappa}+2)}{\eta+2}+1\right)-\frac{(\eta^2+4\eta)y_{(i)}^{2\kappa}+4y_{(i)}^{\kappa}}{(\eta+2)^2}\right], \tag{16}$$

$$F_{\kappa_i}=\frac{\partial F(y_{(i)})}{\partial\kappa}=\eta y_{(i)}^{\kappa}e^{-\eta y_{(i)}^{\kappa}}\log(y_{(i)})\left(\frac{\eta^2y_{(i)}^{2\kappa}+\eta}{\eta+2}\right)\left[(1-\tau)+2\tau e^{-\eta y_{(i)}^{\kappa}}\left(\frac{\eta y_{(i)}^{\kappa}(\eta y_{(i)}^{\kappa}+2)}{\eta+2}+1\right)\right], \tag{17}$$

and

$$F_{\tau_i}=\frac{\partial F(y_{(i)})}{\partial\tau}=\left[1-e^{-\eta y_{(i)}^{\kappa}}\left(\frac{\eta y_{(i)}^{\kappa}(\eta y_{(i)}^{\kappa}+2)}{\eta+2}+1\right)\right]\left[e^{-\eta y_{(i)}^{\kappa}}\left(\frac{\eta y_{(i)}^{\kappa}(\eta y_{(i)}^{\kappa}+2)}{\eta+2}+1\right)\right]. \tag{18}$$

Solving the system of equations $\frac{\partial A(\eta,\kappa,\tau)}{\partial\eta}=0$, $\frac{\partial A(\eta,\kappa,\tau)}{\partial\kappa}=0$, and $\frac{\partial A(\eta,\kappa,\tau)}{\partial\tau}=0$, numerically by using an appropriate approximation yields the ADEs $\hat{\eta}_1$, $\hat{\kappa}_1$, and $\hat{\tau}_1$ of the parameters η, κ, and τ, respectively.

Cramér-von Mises method

Suppose that $y_1, y_2, \dots, y_n$ is a random sample of size n from Tr-PCJD and let $y_{(1)}, y_{(2)}, \dots, y_{(n)}$ represent the corresponding ordered samples. To estimate η, κ, and τ, the CME method (see [30]) involves minimizes the distance between the empirical and theoretical

CDFs for the following function

$$C(\eta,\kappa,\tau)=\frac{1}{12n}+\sum_{i=1}^{n}\left[F(y_{(i)})-\frac{2i-1}{2n}\right]^2.$$

The partial derivatives of $C(\eta,\kappa,\tau)$ with respect to η, κ, and τ, are given, respectively, by:

$$\frac{\partial C(\eta,\kappa,\tau)}{\partial\eta}=2\sum_{i=1}^{n}F_{\eta_i}\left[F_i-\frac{2i-1}{2n}\right],$$

$$\frac{\partial C(\eta,\kappa,\tau)}{\partial\kappa}=2\sum_{i=1}^{n}F_{\kappa_i}\left[F_i-\frac{2i-1}{2n}\right],$$

$$\frac{\partial C(\eta,\kappa,\tau)}{\partial\tau}=2\sum_{i=1}^{n}F_{\tau_i}\left[F_i-\frac{2i-1}{2n}\right],$$

where F_{η_i}, F_{κ_i}, and F_{τ_i} are given in Eqs. (16), (17) and (18). Solving the system of equations $\frac{\partial C(\eta,\kappa,\tau)}{\partial\eta}=0$, $\frac{\partial C(\eta,\kappa,\tau)}{\partial\kappa}=0$, and $\frac{\partial C(\eta,\kappa,\tau)}{\partial\tau}=0$, numerically by using an appropriate approximation yields the CMEs $\hat{\eta}_2$, $\hat{\kappa}_2$, and $\hat{\tau}_2$ of the parameters η, κ, and τ, respectively.

Least squares method

Suppose that $y_1,y_2,\dots,y_n$ be a random sample of size n from the Tr-PCJD and let $y_{(1)},y_{(2)},\dots,y_{(n)}$ represent the corresponding ordered samples. To estimate η, κ, and τ, the LSE (see [31]) involves minimizes the below function:

$$V(\eta,\kappa,\tau)=\sum_{i=1}^{n}\left[F(y_{(i)})-\frac{i}{n+1}\right]^2.$$

The partial derivatives of $V(\eta,\kappa,\tau)$ with respect to η, κ, and τ, are given, respectively, by:

$$\frac{\partial V(\eta,\kappa,\tau)}{\partial\eta}=2\sum_{i=1}^{n}F_{\eta_i}\left[F_i-\frac{i}{n+1}\right],$$

$$\frac{\partial V(\eta,\kappa,\tau)}{\partial\kappa}=2\sum_{i=1}^{n}F_{\kappa_i}\left[F_i-\frac{i}{n+1}\right],$$

$$\frac{\partial V(\eta,\kappa,\tau)}{\partial\tau}=2\sum_{i=1}^{n}F_{\tau_i}\left[F_i-\frac{i}{n+1}\right],$$

where F_{η_i}, F_{κ_i}, and F_{τ_i} are given in Eqs. (16), (17) and (18). Solving the system of equations $\frac{\partial V(\eta,\kappa,\tau)}{\partial\eta}=0$, $\frac{\partial V(\eta,\kappa,\tau)}{\partial\kappa}=0$, and $\frac{\partial V(\eta,\kappa,\tau)}{\partial\tau}=0$, numerically by using an appropriate approximation gives the LSEs $\hat{\eta}_3$, $\hat{\kappa}_3$, and $\hat{\tau}_3$ of the parameters η, κ, and τ, respectively.

Right-tail Anderson–Darling method

Suppose that $y_1,y_2,\dots,y_n$ is a random sample of size n from Tr-PCJD and let $y_{(1)},y_{(2)},\dots,y_{(n)}$ represent the corresponding ordered samples. To estimate η, κ, and τ, the RADE minimizes the following function:

$$R(\eta,\kappa,\tau)=\frac{n}{2}-2\sum_{i=1}^{n}F(y_{(i)})-\frac{1}{n}\sum_{i=1}^{n}(2i-1)\log(1-F(y_{(n-i+1)})).$$

The partial derivatives of $R(\eta,\kappa,\tau)$ with respect to η, κ, and τ, are given, respectively, by:

$$\frac{\partial R(\eta,\kappa,\tau)}{\partial\eta}=-2\sum_{i=1}^{n}F_{\eta_i}+\frac{1}{n}\sum_{i=1}^{n}(2i-1)\frac{F_{\eta_{n-i+1}}}{1-F_{n-i+1}},$$

$$\frac{\partial R(\eta,\kappa,\tau)}{\partial\kappa}=-2\sum_{i=1}^{n}F_{\kappa_i}+\frac{1}{n}\sum_{i=1}^{n}(2i-1)\frac{F_{\kappa_{n-i+1}}}{1-F_{n-i+1}},$$

$$\frac{\partial R(\eta,\kappa,\tau)}{\partial\tau}=-2\sum_{i=1}^{n}F_{\tau_i}+\frac{1}{n}\sum_{i=1}^{n}(2i-1)\frac{F_{\tau_{n-i+1}}}{1-F_{n-i+1}},$$

where F_{η_i}, F_{κ_i}, and F_{τ_i} are given in Eqs. (16), (17) and (18). Solving the system of equations $\frac{\partial R(\eta,\kappa,\tau)}{\partial\eta}=0$, $\frac{\partial R(\eta,\kappa,\tau)}{\partial\kappa}=0$, and $\frac{\partial R(\eta,\kappa,\tau)}{\partial\tau}=0$, numerically by using an appropriate approximation gives the RTADEs $\hat{\eta}_4$, $\hat{\kappa}_4$, and $\hat{\tau}_4$ of the parameters η, κ, and τ, respectively.

Weighted least squares method

Suppose that $y_1, y_2, \ldots, y_n$ is a random sample of size n from Tr-PCJD and let $y_{(1)}, y_{(2)}, \ldots, y_{(n)}$ represent the corresponding ordered samples. To estimate η, κ, and τ, the WLSE minimizes the following function:

$$W(\eta,\kappa,\tau)=\sum_{i=1}^{n}\frac{(n+1)^2(n+2)}{i(n-i+1)}\left[F(y_{(i)})-\frac{i}{n+1}\right]^2.$$

The partial derivatives of $W(\eta,\kappa,\tau)$ with respect to η, κ, and τ, are given, respectively, by:

$$\frac{\partial W(\eta,\kappa,\tau)}{\partial\eta}=2\sum_{i=1}^{n}\frac{(n+1)^2(n+2)F_{\eta_i}}{i(n-i+1)}\left[F_i-\frac{i}{n+1}\right],$$

$$\frac{\partial W(\eta,\kappa,\tau)}{\partial\kappa}=2\sum_{i=1}^{n}\frac{(n+1)^2(n+2)F_{\kappa_i}}{i(n-i+1)}\left[F_i-\frac{i}{n+1}\right],$$

$$\frac{\partial W(\eta,\kappa,\tau)}{\partial\tau}=2\sum_{i=1}^{n}\frac{(n+1)^2(n+2)F_{\tau_i}}{i(n-i+1)}\left[F_i-\frac{i}{n+1}\right],$$

where F_{η_i}, F_{κ_i}, and F_{τ_i} are given in Eqs. (16), (17) and (18). Solving the system of equations $\frac{\partial W(\eta,\kappa,\tau)}{\partial\eta}=0$, $\frac{\partial W(\eta,\kappa,\tau)}{\partial\kappa}=0$, and $\frac{\partial W(\eta,\kappa,\tau)}{\partial\tau}=0$, numerically by using an appropriate approximation gives the WLSEs $\hat{\eta}_5$, $\hat{\kappa}_5$, and $\hat{\tau}_5$ of the parameters η, κ, and τ, respectively.

Anderson–Darling left-tail second order & percentiles

Suppose that $y_1, y_2, \ldots, y_n$ be a random sample of size n from the Tr-PCJD and let $y_{(1)}, y_{(2)}, \ldots, y_{(n)}$ represent the corresponding ordered samples. To estimate η, κ, and τ, the ADTSE minimizes the following function:

$$\mathrm{LTS}(\eta,\kappa,\tau)=2\sum_{i=1}^{n}\log F(y_{(i)})+\frac{1}{n}\sum_{i=1}^{n}\frac{2i-1}{F(y_{(i)})}.$$

The partial derivatives of $\mathrm{LTS}(\eta,\kappa,\tau)$ with respect to η, κ, and τ, are given, respectively, by:

$$\frac{\partial \mathrm{LTS}(\eta,\kappa,\tau)}{\partial\eta}=2\sum_{i=1}^{n}\frac{F_{\eta_i}}{F_i}-\frac{1}{n}\sum_{i=1}^{n}\frac{(2i-1)F_{\eta_i}}{F_i^2},$$

$$\frac{\partial \mathrm{LTS}(\eta,\kappa,\tau)}{\partial\kappa}=2\sum_{i=1}^{n}\frac{F_{\kappa_i}}{F_i}-\frac{1}{n}\sum_{i=1}^{n}\frac{(2i-1)F_{\kappa_i}}{F_i^2},$$

$$\frac{\partial \mathrm{LTS}(\eta,\kappa,\tau)}{\partial\tau}=2\sum_{i=1}^{n}\frac{F_{\tau_i}}{F_i}-\frac{1}{n}\sum_{i=1}^{n}\frac{(2i-1)F_{\tau_i}}{F_i^2},$$

where F_{η_i}, F_{κ_i}, and F_{τ_i} are given in Eqs. (16), (17) and (18). After solving the system of equations $\frac{\partial \mathrm{LTS}(\eta,\kappa,\tau)}{\partial\eta}=0$, $\frac{\partial \mathrm{LTS}(\eta,\kappa,\tau)}{\partial\kappa}=0$, and $\frac{\partial \mathrm{LTS}(\eta,\kappa,\tau)}{\partial\tau}=0$, we get the ADTSE $\hat{\eta}_6$, $\hat{\kappa}_6$, and $\hat{\tau}_6$ of the parameters η, κ, and τ, respectively estimates of η, κ, and τ.

To estimate η, κ, and τ, of the Tr-PCJD, the PE minimizes the following function:

$$\mathrm{PE}(\eta,\kappa,\tau)=\sum_{i=1}^{n}\left[y_{(i)}-Q(\eta,\kappa,\tau)\right]^2,$$

with respect to η, κ, and τ.

Simulation

We conducted a comprehensive simulation study to evaluate and compare the performance of the eight different estimators applied to the Tr-PCJD parameters. We used R software (R 4.3.2), by generating 1000 samples from Tr-PCJD, with sample sizes { 30, 50, 150, 300, 450 }, and with initial values of the parameters (η,κ,τ) = (0.4, 0.8, 0.9), (0.8, 1.2, 0.3), (0.8, 1.9, 0.9), (1.4, 0.4, 0.3), (1.4, 0.4, 0.7) and (2.0, 0.8, 0.7). For every sample and parameter combination, we determine the following metrics: the mean and the mean squared error (MSE) of the estimates. To establish a guideline for selecting the most effective estimation method for the Tr-PCJD parameters, we computed both the partial and overall rankings of all estimation methods for each parameter combinations. Tables from 4 to 9 display the mean and MSE for the MLE, ADE, CME, LSE, RADE, WLSE, ADLTSE, and PE. Additionally, these tables assign a rank to each estimator within each row, indicated by superscripts. Table 10 presents the partial and overall ranks of the various estimation methods in all parameters. The MSE outcomes presented in Table 4 are visually graphed in Figs. 2 to 4. Fig. 2 graphically depicts the MSE for η estimates, Fig. 3 showcases the MSE for κ estimates, and Fig. 4 represents the MSE for τ estimates. These figures, using eight different methods, provide a visual representation of how the estimates' performance evolves as the sample size increases.

Examining the tables from Tables 4 to 9, together with Table 10 and Figs. 2–4, we observe the following:

Table 4
Results for estimation methods considering $\eta = 0.4$, $\kappa = 0.8$, and $\tau = 0.9$.

n	Parameter	Estimate	MLE	ADE	CME	LSE	RADE	WLSE	ADLTSE	PE
30	η	Mean	0.4366	0.4132	0.4081	0.4083	0.4106	0.4075	0.4166	0.4140
		MSE	0.0134[5]	0.0115[1]	0.0135[7]	0.0135[6]	0.0118[4]	0.0136[8]	0.0118[3]	0.0115[2]
	κ	Mean	0.8634	0.7958	0.8120	0.8122	0.7932	0.8109	0.7996	0.7985
		MSE	0.0157[4]	0.0144[2]	0.0178[7]	0.0178[6]	0.0160[5]	0.0181[8]	0.0145[3]	0.0139[1]
	τ	Mean	0.5516	0.9820	0.9842	0.9768	1.0081	1.0118	0.9365	0.9529
		MSE	0.1488[1]	0.4403[6]	0.4619[7]	0.4075[4]	0.3709[3]	0.7442[8]	0.4268[5]	0.3194[2]
50	η	Mean	0.4244	0.4106	0.4084	0.4084	0.4060	0.4084	0.4114	0.4104
		MSE	0.0076[5]	0.0068[3]	0.0085[7]	0.0085[7]	0.0066[1]	0.0085[7]	0.0068[4]	0.0068[2]
	κ	Mean	0.8507	0.8017	0.8092	0.8092	0.7989	0.8092	0.8023	0.8023
		MSE	0.0087[1]	0.0089[3]	0.0110[7]	0.0110[7]	0.0095[5]	0.0110[7]	0.0089[4]	0.0088[2]
	τ	Mean	0.5986	0.8829	0.8982	0.8982	0.9257	0.8982	0.8740	0.8813
		MSE	0.1313[1]	0.1817[5]	0.2598[7]	0.2598[7]	0.1710[2]	0.2598[7]	0.1729[3]	0.1794[4]
150	η	Mean	0.4227	0.4156	0.4165	0.4165	0.4094	0.4165	0.4156	0.4156
		MSE	0.0038[5]	0.0035[2.5]	0.0047[7]	0.0047[7]	0.0029[1]	0.0047[7]	0.0035[2.5]	0.0035[4]
	κ	Mean	0.8301	0.8097	0.8090	0.8090	0.8081	0.8090	0.8097	0.8098
		MSE	0.0031[4]	0.0031[1.5]	0.0040[7]	0.0040[7]	0.0034[5]	0.0040[7]	0.0031[1.5]	0.0031[3]
	τ	Mean	0.6652	0.7911	0.8050	0.8050	0.8325	0.8050	0.7911	0.7910
		MSE	0.1095[5]	0.0935[2.5]	0.1458[7]	0.1458[7]	0.0635[1]	0.1458[7]	0.0935[2.5]	0.0936[4]
300	η	Mean	0.4158	0.4131	0.4148	0.4148	0.4088	0.4148	0.4131	0.4130
		MSE	0.0028[8]	0.0020[3.5]	0.0028[6]	0.0028[6]	0.0017[1]	0.0028[6]	0.0020[3.5]	0.0020[2]
	κ	Mean	0.8175	0.8059	0.8042	0.8042	0.8062	0.8042	0.8059	0.8059
		MSE	0.0017[4]	0.0016[1.5]	0.0022[7]	0.0022[7]	0.0018[5]	0.0022[7]	0.0016[1.5]	0.0016[3]
	τ	Mean	0.7582	0.8147	0.8208	0.8208	0.8382	0.8208	0.8147	0.8152
		MSE	0.0836[5]	0.0721[3.5]	0.1126[7]	0.1126[7]	0.0543[1]	0.1126[7]	0.0721[3.5]	0.0719[2]
450	η	Mean	0.4125	0.4127	0.4140	0.4140	0.4078	0.4140	0.4127	0.4127
		MSE	0.0022[5]	0.0018[3]	0.0023[7]	0.0023[7]	0.0014[1]	0.0023[7]	0.0018[3]	0.0018[3]
	κ	Mean	0.8113	0.8061	0.8040	0.8040	0.8051	0.8040	0.8061	0.8061
		MSE	0.0018[8]	0.0013[2]	0.0016[6]	0.0016[6]	0.0013[4]	0.0016[6]	0.0013[2]	0.0013[2]
	τ	Mean	0.7864	0.8056	0.8131	0.8131	0.8368	0.8131	0.8056	0.8056
		MSE	0.0818[5]	0.0740[3]	0.1023[7]	0.1023[7]	0.0534[1]	0.1023[7]	0.0740[3]	0.0740[3]

- MSE decreases as the sample size increases, which means that all estimation methods are consistent.
- Most methods tend to overestimate η.
- RADE shows superiority, as it has the lowest rank for MSE.
- MLE is the second preferable method with respect to rank followed by ADLTS and ADE.

Applications

The significance and promise of the Tr-PCJD distribution are demonstrated in this section through the use of three real data sets.

The first data set represents values for inflation rate in several countries recorded in June 2024. The term “inflation rate” describes how prices for products and services vary over time. The electronic address from which it was taken is as follows: https://tradingeconomics.com/. The data set is reported in Table 11.

The second data set represents the remission time in months of 128 bladder cancer patients. The data were taken from [32]. The data set values are 2.54, 11.79, 14.83, 1.4, 14.77, 12.03, 11.98, 5.85, 5.71, 4.87, 8.37, 14.76, 5.17, 7.63, 3.7, 2.69, 2.02, 2.23, 8.53, 4.23, 0.5, 14.24, 3.52, 2.09, 2.02, 3.02, 7.26, 2.46, 10.34, 1.26, 0.81, 25.82, 43.01, 9.02, 13.29, 5.09, 10.06, 6.76, 2.69, 4.98, 6.25, 1.19, 10.66, 11.25, 11.64, 5.62, 79.05, 6.94, 4.33, 6.54, 2.62, 46.12, 17.12, 2.64, 32.15, 1.05, 36.66, 4.34, 16.62, 4.26, 5.32, 6.93, 9.22, 4.18, 13.11, 2.26, 3.36, 8.66, 0.9, 8.65, 5.41, 1.76, 26.31, 7.93, 7.09, 3.88, 3.64, 5.49, 0.51, 12.07, 7.32, 7.39, 9.47, 18.1, 0.4, 12.02, 20.28, 7.59, 17.14, 19.13, 4.4, 3.82, 3.31, 2.83, 34.26, 10.75, 9.74, 5.06, 3.48, 7.66, 5.34, 7.28, 1.35, 2.75, 2.07, 7.87, 13.8, 0.2, 5.41, 6.97, 15.96, 21.73, 12.63, 7.62, 3.36, 22.69, 0.08, 25.74, 1.46, 4.51, 3.57, 17.36, 3.25, 5.32, 23.63, 2.87, 4.5, 8.26.

The third data point represents the percentage of 211 countries of global CO_2 emissions per person in 2020. The data were previously used in [33] and are given as follows: 37.02, 30.45, 26.98, 25.37, 23.22, 20.83, 20.55, 20.32, 17.97, 15.52, 15.37, 15.19, 14.24, 14.2, 14, 13.06, 12.49, 12.17, 12.12, 11.66, 11.47, 10.81, 10.03, 9.06, 8.87, 8.74, 8.6, 8.42, 8.23, 8.22, 8.15, 8.06, 7.92, 7.88, 7.78, 7.69, 7.62, 7.62, 7.41, 7.38, 7.32, 7.23, 7.09, 7.05, 6.98, 6.94, 6.75, 6.73, 6.53, 6.51, 6.4, 6.26, 6.08, 6.04, 6.03, 5.94, 5.63, 5.39, 5.38, 5.24, 5.24, 5.23, 5.07, 5.07, 5.02, 5.01, 5, 4.99, 4.94, 4.89, 4.85, 4.66, 4.65, 4.61, 4.52, 4.52, 4.47, 4.4, 4.25, 4.24, 4.14, 3.99, 3.96, 3.83, 3.8, 3.79, 3.78, 3.73, 3.72, 3.72, 3.7, 3.69, 3.68, 3.61, 3.59, 3.53, 3.47, 3.43, 3.37, 3.32, 3.13, 2.98, 2.95, 2.81, 2.77, 2.77, 2.62, 2.61, 2.56, 2.56, 2.51, 2.5, 2.5, 2.5, 2.5, 2.44, 2.4, 2.38, 2.36, 2.2, 2.16, 2.09, 1.99, 1.94, 1.93, 1.93,

Table 5
Results for estimation methods considering $\eta = 0.8$, $\kappa = 1.2$, and $\tau = 0.3$.

n	Parameter	Estimate	MLE	ADE	CME	LSE	RADE	WLSE	ADLTSE	PE
30	η	Mean	0.839892	0.856285	0.834078	0.833694	0.815437	0.833523	0.847026	0.855608
		MSE	0.0432[2]	0.0539[7]	0.0451[3]	0.0454[5]	0.0370[1]	0.0453[4]	0.0515[6]	0.0541[8]
	κ	Mean	1.226657	1.17996	1.21089	1.210261	1.200688	1.210338	1.182492	1.179555
		MSE	0.0257[1]	0.0273[4]	0.0339[6]	0.0342[8]	0.0265[2]	0.0342[7]	0.0272[3]	0.0275[5]
	τ	Mean	0.182734	0.223642	0.243029	0.243485	0.289771	0.243029	0.24227	0.223985
		MSE	0.1378[1]	0.1873[7]	0.1720[4.5]	0.1719[3]	0.1469[2]	0.1720[4.5]	0.1778[6]	0.1873[8]
50	η	Mean	0.851297	0.852852	0.834572	0.834572	0.821346	0.834572	0.850005	0.852911
		MSE	0.0385[5]	0.0462[7]	0.0378[3]	0.0378[3]	0.0316[1]	0.0378[3]	0.0455[6]	0.0463[8]
	κ	Mean	1.20397	1.175947	1.200261	1.200261	1.188298	1.200261	1.177233	1.175981
		MSE	0.0162[1]	0.0202[4]	0.0243[7]	0.0243[7]	0.0176[2]	0.0243[7]	0.0200[3]	0.0202[5]
	τ	Mean	0.191323	0.244659	0.259818	0.259818	0.300005	0.259818	0.251031	0.244325
		MSE	0.1382[5]	0.1662[7]	0.1375[3]	0.1375[3]	0.1271[1]	0.1375[3]	0.1636[6]	0.1663[8]
150	η	Mean	0.843704	0.851007	0.849167	0.849167	0.837802	0.849167	0.851007	0.851303
		MSE	0.0258[5]	0.0301[6.5]	0.0243[3]	0.0243[3]	0.0219[1]	0.0243[3]	0.0301[6.5]	0.0302[8]
	κ	Mean	1.192886	1.17592	1.181493	1.181493	1.178195	1.181493	1.17592	1.175938
		MSE	0.0064[2]	0.0078[3.5]	0.0081[7]	0.0081[7]	0.0061[1]	0.0081[7]	0.0078[3.5]	0.0079[5]
	τ	Mean	0.215953	0.228383	0.220813	0.220813	0.25524	0.220813	0.228383	0.22751
		MSE	0.1163[5]	0.1305[6.5]	0.1126[2]	0.1126[2]	0.1153[4]	0.1126[2]	0.1305[6.5]	0.1307[8]
300	η	Mean	0.839828	0.850104	0.845627	0.845627	0.836387	0.845627	0.850104	0.850202
		MSE	0.0201[2]	0.0270[6.5]	0.0231[4]	0.0231[4]	0.0200[1]	0.0231[4]	0.0270[6.5]	0.0271[8]
	κ	Mean	1.191857	1.175974	1.179635	1.179635	1.179008	1.179635	1.175974	1.175994
		MSE	0.0041[2]	0.0056[6.5]	0.0056[4]	0.0056[4]	0.0041[1]	0.0056[4]	0.0056[6.5]	0.0056[8]
	τ	Mean	0.223966	0.228926	0.233796	0.233796	0.257973	0.233796	0.228926	0.22848
		MSE	0.0976[1]	0.1250[7.5]	0.1116[4]	0.1116[4]	0.1086[2]	0.1116[4]	0.1250[7.5]	0.1250[6]
450	η	Mean	0.836617	0.84597	0.85044	0.85044	0.840846	0.85044	0.84597	0.846005
		MSE	0.0156[1]	0.0220[6.5]	0.0218[4]	0.0218[4]	0.0183[2]	0.0218[4]	0.0220[6.5]	0.0220[8]
	κ	Mean	1.192319	1.177178	1.175935	1.175935	1.176761	1.175935	1.177178	1.177236
		MSE	0.0029[1]	0.0043[4.5]	0.0047[7]	0.0047[7]	0.0033[2]	0.0047[7]	0.0043[4.5]	0.0043[3]
	τ	Mean	0.223552	0.229941	0.219899	0.219899	0.242471	0.219899	0.229941	0.229816
		MSE	0.0816[1]	0.1085[6.5]	0.1063[4]	0.1063[4]	0.1033[2]	0.1063[4]	0.1085[6.5]	0.1086[8]

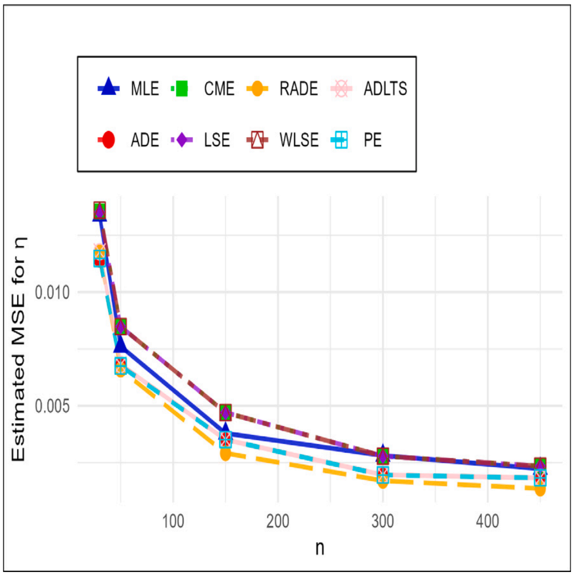

Fig. 2. Estimated MSE for η in Table 4.

Table 6
Results for estimation methods considering $\eta = 0.8$, $\kappa = 1.9$, and $\tau = 0.9$.

n	Parameter	Estimate	MLE	ADE	CME	LSE	RADE	WLSE	ADLTSE	PE
30	η	Mean	0.927031	0.812241	0.80719	0.809042	0.819442	0.804752	0.824422	0.814946
		MSE	0.0514[8]	0.0325[2]	0.0417[5]	0.0410[4]	0.0417[6]	0.0426[7]	0.0317[1]	0.0325[3]
	κ	Mean	2.031525	1.879399	1.929335	1.931308	1.886995	1.925904	1.887844	1.884099
		MSE	0.0948[1]	0.0965[3]	0.1373[7]	0.1368[6]	0.1070[5]	0.1388[8]	0.0970[4]	0.0955[2]
	τ	Mean	0.53202	1.002958	1.041285	1.01844	0.983304	1.079343	0.977963	0.998499
		MSE	0.1888[1]	0.3801[2]	0.6175[7]	0.4711[4]	0.4453[3]	0.9390[8]	0.5490[6]	0.5003[5]
50	η	Mean	0.896979	0.828697	0.824472	0.824428	0.8256	0.822792	0.832947	0.829515
		MSE	0.0315[8]	0.0248[4]	0.0299[6]	0.0296[5]	0.0238[2]	0.0307[7]	0.0237[1]	0.0239[3]
	κ	Mean	2.027593	1.912574	1.938269	1.939415	1.911407	1.936559	1.91631	1.91553
		MSE	0.0617[1]	0.0637[4]	0.0850[7]	0.0844[6]	0.0679[5]	0.0857[8]	0.0636[3]	0.0627[2]
	τ	Mean	0.576157	0.877343	0.905069	0.900655	0.883941	0.934558	0.858858	0.866745
		MSE	0.1516[2]	0.1880[5]	0.2777[7]	0.2523[6]	0.1634[4]	0.5709[8]	0.1573[3]	0.1510[1]
150	η	Mean	0.886818	0.835616	0.830031	0.830031	0.828064	0.830031	0.835616	0.835689
		MSE	0.0221[8]	0.0150[2.5]	0.0180[6]	0.0180[6]	0.0124[1]	0.0180[6]	0.0150[2.5]	0.0150[4]
	κ	Mean	1.970647	1.914873	1.910584	1.910584	1.914299	1.910584	1.914873	1.914711
		MSE	0.0200[1]	0.0216[4.5]	0.0284[7]	0.0284[7]	0.0215[2]	0.0284[7]	0.0216[4.5]	0.0216[3]
	τ	Mean	0.632591	0.815141	0.850289	0.850289	0.834189	0.850289	0.815141	0.815111
		MSE	0.1351[8]	0.0860[2.5]	0.1340[6]	0.1340[6]	0.0688[1]	0.1340[6]	0.0860[2.5]	0.0861[4]
300	η	Mean	0.862094	0.831072	0.831886	0.831886	0.82301	0.831886	0.831072	0.831072
		MSE	0.0162[8]	0.0098[3]	0.0140[6]	0.0140[6]	0.0082[1]	0.0140[6]	0.0098[3]	0.0098[3]
	κ	Mean	1.949112	1.913468	1.906715	1.906715	1.911612	1.906715	1.913468	1.913468
		MSE	0.0114[1]	0.0115[3]	0.0155[7]	0.0155[7]	0.0116[5]	0.0155[7]	0.0115[3]	0.0115[3]
	τ	Mean	0.711968	0.818019	0.832901	0.832901	0.839884	0.832901	0.818019	0.818019
		MSE	0.1068[8]	0.0672[3]	0.1050[6]	0.1050[6]	0.0536[1]	0.1050[6]	0.0672[3]	0.0672[3]
450	η	Mean	0.859186	0.831847	0.836619	0.837194	0.82222	0.837194	0.831847	0.831824
		MSE	0.0184[8]	0.0082[2.5]	0.0126[5]	0.0129[6.5]	0.0065[1]	0.0129[6.5]	0.0082[2.5]	0.0082[4]
	κ	Mean	1.932635	1.917219	1.912374	1.912234	1.914147	1.912234	1.917219	1.917154
		MSE	0.0092[5]	0.0079[1.5]	0.0105[6]	0.0105[7.5]	0.0083[4]	0.0105[7.5]	0.0079[1.5]	0.0079[3]
	τ	Mean	0.736163	0.812978	0.812501	0.811219	0.840003	0.811219	0.812978	0.813174
		MSE	0.1109[8]	0.0618[2.5]	0.0958[5]	0.0976[6.5]	0.0467[1]	0.0976[6.5]	0.0618[2.5]	0.0619[4]

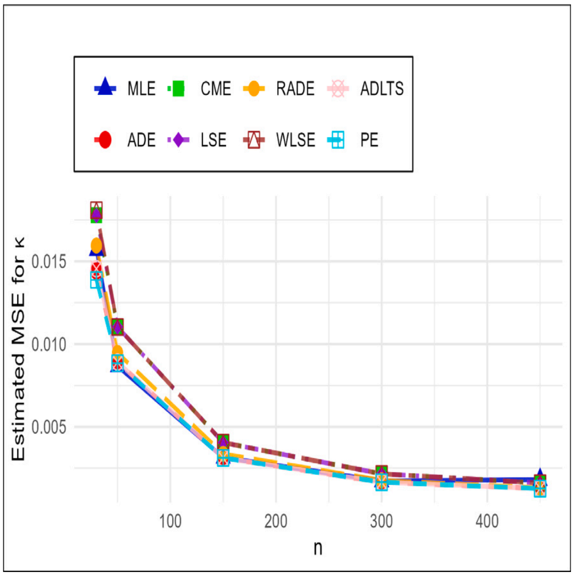

Fig. 3. Estimated MSE for κ in Table 4.

Table 7
Results for estimation methods considering $\eta = 1.4$, $\kappa = 0.4$, and $\tau = 0.3$.

n	Parameter	Estimate	MLE	ADE	CME	LSE	RADE	WLSE	ADLTSE	PE
30	η	Mean	1.421165	1.43338	1.452252	1.450641	1.394509	1.45076	1.429137	1.439633
		MSE	0.0727[1]	0.1046[8]	0.0993[3]	0.1008[5]	0.0888[2]	0.1008[4]	0.1041[7]	0.1034[6]
	κ	Mean	0.421592	0.39911	0.408251	0.408279	0.404694	0.407985	0.399163	0.398292
		MSE	0.0037[1]	0.0038[3]	0.0056[6]	0.0056[7]	0.0043[5]	0.0056[8]	0.0038[4]	0.0038[2]
	τ	Mean	0.244998	0.280585	0.246479	0.247425	0.322775	0.24716	0.289145	0.26499
		MSE	0.1058[1]	0.1810[8]	0.1583[5]	0.1582[4]	0.1491[2]	0.1581[3]	0.1777[6]	0.1796[7]
50	η	Mean	1.385246	1.416998	1.442956	1.442956	1.403675	1.442956	1.416488	1.413929
		MSE	0.0530[1]	0.0776[5]	0.0790[7]	0.0790[7]	0.0658[2]	0.0790[7]	0.0775[4]	0.0765[3]
	κ	Mean	0.419361	0.401974	0.404698	0.404698	0.402054	0.404698	0.402028	0.402297
		MSE	0.0021[1]	0.0023[2]	0.0031[7]	0.0031[7]	0.0023[5]	0.0031[7]	0.0023[3]	0.0023[4]
	τ	Mean	0.308014	0.29567	0.260628	0.260628	0.313479	0.260628	0.296487	0.297249
		MSE	0.0844[1]	0.1360[8]	0.1318[4]	0.1318[4]	0.1119[2]	0.1318[4]	0.1357[7]	0.1341[6]
150	η	Mean	1.336547	1.374933	1.416265	1.416265	1.390663	1.416265	1.374933	1.374831
		MSE	0.0286[1]	0.0448[6.5]	0.0436[3]	0.0436[3]	0.0439[5]	0.0436[3]	0.0448[6.5]	0.0451[8]
	κ	Mean	0.414786	0.402455	0.400192	0.400192	0.398239	0.400192	0.402455	0.402248
		MSE	0.0008[1]	0.0009[3.5]	0.0011[7]	0.0011[7]	0.0009[2]	0.0011[7]	0.0009[3.5]	0.0009[5]
	τ	Mean	0.366299	0.335116	0.274564	0.274564	0.317633	0.274564	0.335116	0.33472
		MSE	0.0614[1]	0.1020[5.5]	0.0982[3]	0.0982[3]	0.1047[8]	0.0982[3]	0.1020[5.5]	0.1025[7]
300	η	Mean	1.316292	1.349147	1.392008	1.392008	1.388364	1.392008	1.349147	1.349147
		MSE	0.0218[1]	0.0345[3]	0.0375[6]	0.0375[6]	0.0421[8]	0.0375[6]	0.0345[3]	0.0345[3]
	κ	Mean	0.416391	0.406682	0.403871	0.403871	0.399874	0.403871	0.406682	0.406682
		MSE	0.0005[5]	0.0005[3]	0.0006[7]	0.0006[7]	0.0005[1]	0.0006[7]	0.0005[3]	0.0005[3]
	τ	Mean	0.411403	0.383671	0.323363	0.323363	0.336217	0.323363	0.383671	0.383671
		MSE	0.0479[1]	0.0814[3]	0.0855[6]	0.0855[6]	0.0944[8]	0.0855[6]	0.0814[3]	0.0814[3]
450	η	Mean	1.329133	1.370123	1.397774	1.397774	1.433986	1.397774	1.370123	1.370123
		MSE	0.0176[1]	0.0359[3]	0.0404[6]	0.0404[6]	0.0457[8]	0.0404[6]	0.0359[3]	0.0359[3]
	κ	Mean	0.415318	0.404973	0.401287	0.401287	0.397637	0.401287	0.404973	0.404973
		MSE	0.0004[2]	0.0004[4]	0.0005[7]	0.0005[7]	0.0004[1]	0.0005[7]	0.0004[4]	0.0004[4]
	τ	Mean	0.379904	0.340988	0.305104	0.305104	0.252704	0.305104	0.340988	0.340988
		MSE	0.0276[1]	0.0669[3]	0.0757[6]	0.0757[6]	0.0860[8]	0.0757[6]	0.0669[3]	0.0669[3]

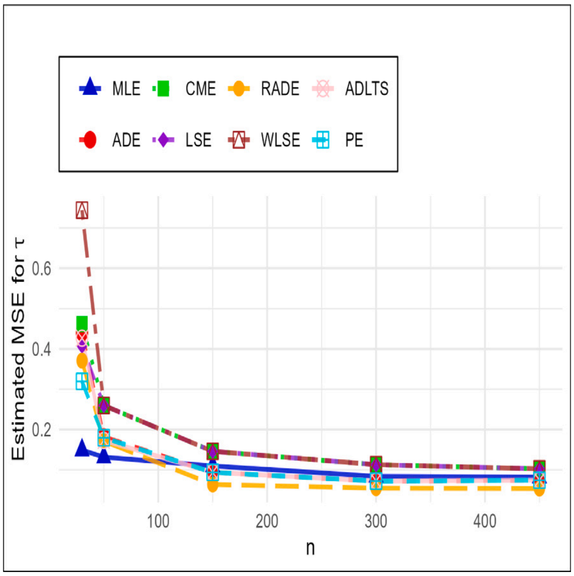

Fig. 4. Estimated MSE for τ in Table 4.

Table 8
Results for estimation methods considering $\eta = 1.4$, $\kappa = 0.4$ and $\tau = 0.7$.

n	Parameter	Estimate	MLE	ADE	CME	LSE	RADE	WLSE	ADLTSE	PE
30	η	Mean	1.546381	1.306723	1.307871	1.312278	1.28529	1.303076	1.306049	1.28472
		MSE	0.0804[1]	0.1024[3]	0.1210[7]	0.1171[6]	0.1004[2]	0.1257[8]	0.1058[4]	0.1106[5]
	κ	Mean	0.431549	0.404085	0.413619	0.414316	0.394756	0.412716	0.403193	0.406552
		MSE	0.0048[3]	0.0047[1]	0.0073[7]	0.0072[6]	0.0052[5]	0.0074[8]	0.0047[2]	0.0051[4]
	τ	Mean	0.503385	0.924399	0.974843	0.950396	0.961173	1.015822	0.963387	0.988492
		MSE	0.0696[1]	0.3386[3]	0.4946[5]	0.3689[4]	0.3027[2]	0.8664[8]	0.7846[7]	0.6680[6]
50	η	Mean	1.514608	1.360275	1.351844	1.351844	1.317792	1.35027	1.361451	1.35389
		MSE	0.0554[1]	0.0574[3]	0.0784[6.5]	0.0784[6.5]	0.0618[5]	0.0799[8]	0.0571[2]	0.0590[4]
	κ	Mean	0.422086	0.404216	0.407423	0.407423	0.392432	0.40719	0.404158	0.405641
		MSE	0.0024[1]	0.0026[2]	0.0044[6.5]	0.0044[6.5]	0.0031[5]	0.0044[8]	0.0026[3]	0.0027[4]
	τ	Mean	0.526023	0.784308	0.843795	0.843795	0.868772	0.855496	0.782164	0.792831
		MSE	0.0624[1]	0.1098[3]	0.2235[6.5]	0.2235[6.5]	0.1556[5]	0.3084[8]	0.1083[2]	0.1115[4]
150	η	Mean	1.477844	1.397796	1.375323	1.375323	1.369093	1.375323	1.397796	1.397708
		MSE	0.0322[5]	0.0252[2.5]	0.0339[7]	0.0339[7]	0.0248[1]	0.0339[7]	0.0252[2.5]	0.0253[4]
	κ	Mean	0.416759	0.407594	0.406033	0.406033	0.399457	0.406033	0.407594	0.4076
		MSE	0.0009[1]	0.0009[2.5]	0.0013[7]	0.0013[7]	0.0010[5]	0.0013[7]	0.0009[2.5]	0.0009[4]
	τ	Mean	0.580908	0.712205	0.766274	0.766274	0.764076	0.766274	0.712205	0.712429
		MSE	0.0506[5]	0.0431[1.5]	0.0781[7]	0.0781[7]	0.0499[4]	0.0781[7]	0.0431[1.5]	0.0433[3]
300	η	Mean	1.480429	1.421186	1.407455	1.407455	1.38673	1.407455	1.421186	1.421186
		MSE	0.0187[4]	0.0169[2]	0.0197[6]	0.0197[6]	0.0231[8]	0.0197[6]	0.0169[2]	0.0169[2]
	κ	Mean	0.420026	0.411877	0.41016	0.41016	0.401744	0.41016	0.411877	0.411877
		MSE	0.0006[5]	0.0006[3]	0.0008[7]	0.0008[7]	0.0005[1]	0.0008[7]	0.0006[3]	0.0006[3]
	τ	Mean	0.555246	0.657264	0.690076	0.690076	0.7245	0.690076	0.657264	0.657264
		MSE	0.0446[7]	0.0358[2]	0.0419[5]	0.0419[5]	0.0494[8]	0.0419[5]	0.0358[2]	0.0358[2]
450	η	Mean	1.457456	1.395922	1.39152	1.39152	1.380319	1.39152	1.395922	1.395922
		MSE	0.0377[8]	0.0178[3]	0.0225[6]	0.0225[6]	0.0140[1]	0.0225[6]	0.0178[3]	0.0178[3]
	κ	Mean	0.418207	0.415784	0.416789	0.416789	0.409306	0.416789	0.415784	0.415784
		MSE	0.0005[5]	0.0005[3]	0.0007[7]	0.0007[7]	0.0004[1]	0.0007[7]	0.0005[3]	0.0005[3]
	τ	Mean	0.587932	0.691196	0.710419	0.710419	0.720026	0.710419	0.691196	0.691196
		MSE	0.0780[8]	0.0254[2]	0.0419[6]	0.0419[6]	0.0262[4]	0.0419[6]	0.0254[2]	0.0254[2]

1.88, 1.78, 1.77, 1.77, 1.76, 1.75, 1.75, 1.75, 1.74, 1.68, 1.58, 1.56, 1.55, 1.55, 1.53, 1.47, 1.36, 1.36, 1.28, 1.24, 1.24, 1.14, 1.06, 1.06, 1.06, 1.02, 0.99, 0.99, 0.99, 0.98, 0.94, 0.92, 0.82, 0.77, 0.74, 0.73, 0.71, 0.68, 0.67, 0.64, 0.62, 0.61, 0.59, 0.58, 0.57, 0.56, 0.56, 0.55, 0.51, 0.51, 0.43, 0.43, 0.4, 0.38, 0.36, 0.36, 0.33, 0.31, 0.3, 0.3, 0.26, 0.26, 0.26, 0.26, 0.21, 0.21, 0.2, 0.2, 0.19, 0.18, 0.17, 0.15, 0.13, 0.13, 0.11, 0.11, 0.11, 0.08, 0.07, 0.07, 0.06, 0.05, 0.04, 0.04, 0.03

The descriptive analysis of all data sets is reported in Table 12.

The actual datasets are used to evaluate the adequacy of the Tr-PCJD distribution's fit. The Tr-PCJD distribution is compared with XLD [34], KwLD [35], KwCJD [23], WPLD [36], WLD [37], EGXLD [38], and PCJD.

Calculations are made to determine the MLEs and standard errors (SEs) of the model parameters. Several criteria are taken into account to evaluate the distribution models. These criteria include the Akaike information criterion (W_1), the correct Akaike information criterion (W_2), the Hannan–Quinn information criterion (W_3), the Kolmogorov–Smirnov test (W_4), its p-value (W_5), the CM test (W_6), its p-value (W_7), the AD test (W_8) and its p-value (W_9) test. This contrasts to the larger dispersion, which is related to lower values of W_1, W_2, W_3, W_4, W_6, and W_8, as well as the maximum magnitude of W_5, W_7 and W_9. The MLEs of the competing models, together with their SEs and values of W_i, $i = 1,2,3,4,5,6,7,8,9$ for the recommended data sets, are presented in Tables 13, 14, 16, 17, 19, 20.

Compared to other models, the Tr-PCJD, defined by three parameters, has been shown to demonstrate a higher degree of goodness of fit. Among the distributions that are being taken into account for this study, this particular distribution has the most incredible value of W_5 and the lowest values of W_1, W_2, W_3, W_4, W_6 and W_8. Furthermore, this distribution has the lowest value of W_7 and W_9.

The MLEs, LSEs, WLSEs, CMEs, ADEs, RADEs, PEs and ADLTSE estimation methods are utilized to estimate the Tr-PCJD parameters from the data sets. The estimates and the values of W_4 statistic with its W_5 are reported in Tables 15–21. The W_4 and W_5 in Table 15 make it clear that the LSEs are advised to estimate the parameters for data set 1. According to Table 18's data set 2, using WLSEs is advised for estimating parameters. Furthermore, according to Table 21, data set 3 suggests using ADEs to estimate parameters.

Furthermore, Figs. 5–7 include the histogram, violin plot, QQ (quantile–quantile) plot, and TTT (total time in test) plot. The estimated PDFs of competing models for the datasets are shown in Figs. 8, 14, 20, while Figs. 9, 15, 21 display the estimated CDFs of the competitive models. Furthermore, Figs. 10, 16, 22 illustrate the PP plots of the competing models. A visual comparison of

Table 9
Results for estimation methods considering $\eta = 2$, $\kappa = 0.8$ and $\tau = 0.7$.

n	Parameter	Estimate	MLE	ADE	CME	LSE	RADE	WLSE	ADLTSE	PE
30	η	Mean	2.271449	2.136432	2.162408	2.16958	2.103991	2.162694	2.136943	2.137602
		MSE	0.1907[1]	0.2374[4]	0.2903[8]	0.2835[6]	0.1958[2]	0.2887[7]	0.2410[5]	0.2303[3]
	κ	Mean	0.815523	0.788075	0.812449	0.813825	0.786314	0.81272	0.785888	0.789652
		MSE	0.0143[1]	0.0187[2]	0.0275[7]	0.0274[6]	0.0196[5]	0.0276[8]	0.0188[4]	0.0188[3]
	τ	Mean	0.399381	0.63716	0.675729	0.655602	0.664052	0.674508	0.650293	0.629452
		MSE	0.1858[1]	0.3587[5]	0.4287[7]	0.3394[2]	0.3473[4]	0.4246[6]	0.4553[8]	0.3468[3]
50	η	Mean	2.27966	2.12052	2.113755	2.113755	2.122204	2.113755	2.124579	2.122153
		MSE	0.1927[5]	0.1712[4]	0.1942[7]	0.1942[7]	0.1378[1]	0.1942[7]	0.1681[2]	0.1684[3]
	κ	Mean	0.81165	0.793364	0.809934	0.809934	0.794894	0.809934	0.793736	0.793656
		MSE	0.0100[1]	0.0121[4]	0.0173[7]	0.0173[7]	0.0119[2]	0.0173[7]	0.0121[5]	0.0120[3]
	τ	Mean	0.406966	0.599764	0.647286	0.647286	0.590358	0.647286	0.594942	0.594582
		MSE	0.1925[2]	0.2238[5]	0.2448[7]	0.2448[7]	0.1775[1]	0.2448[7]	0.2167[4]	0.2050[3]
150	η	Mean	2.244374	2.085199	2.053117	2.053117	2.105085	2.053117	2.085199	2.085358
		MSE	0.1578[8]	0.1138[2.5]	0.1344[6]	0.1344[6]	0.1127[1]	0.1344[6]	0.1138[2.5]	0.1139[4]
	κ	Mean	0.801066	0.791678	0.792357	0.792357	0.788828	0.792357	0.791678	0.791724
		MSE	0.0033[1]	0.0038[3.5]	0.0051[7]	0.0051[7]	0.0038[2]	0.0051[7]	0.0038[3.5]	0.0038[5]
	τ	Mean	0.469475	0.62969	0.680613	0.680613	0.607087	0.680613	0.62969	0.62933
		MSE	0.1501[5]	0.1255[1.5]	0.1525[7]	0.1525[7]	0.1268[4]	0.1525[7]	0.1255[1.5]	0.1256[3]
300	η	Mean	2.235282	2.086996	2.048876	2.048876	2.12234	2.048876	2.086996	2.086996
		MSE	0.1436[8]	0.0885[2]	0.1002[5]	0.1002[5]	0.1051[7]	0.1002[5]	0.0885[2]	0.0885[2]
	κ	Mean	0.802953	0.797641	0.79709	0.79709	0.792019	0.79709	0.797641	0.797641
		MSE	0.0019[1]	0.0020[3]	0.0030[7]	0.0030[7]	0.0021[5]	0.0030[7]	0.0020[3]	0.0020[3]
	τ	Mean	0.480782	0.627209	0.678138	0.678138	0.589788	0.678138	0.627209	0.627209
		MSE	0.1326[8]	0.0876[2]	0.1018[5]	0.1018[5]	0.1050[7]	0.1018[5]	0.0876[2]	0.0876[2]
450	η	Mean	2.235812	2.05914	2.019845	2.019845	2.107674	2.019845	2.05914	2.059023
		MSE	0.1324[8]	0.0716[1.5]	0.0797[5]	0.0797[5]	0.0907[7]	0.0797[5]	0.0716[1.5]	0.0716[3]
	κ	Mean	0.801085	0.794977	0.793282	0.793282	0.790861	0.793282	0.794977	0.794943
		MSE	0.0014[1]	0.0015[2.5]	0.0021[7]	0.0021[7]	0.0016[5]	0.0021[7]	0.0015[2.5]	0.0015[4]
	τ	Mean	0.482651	0.65457	0.702681	0.702681	0.605331	0.702681	0.65457	0.654567
		MSE	0.1221[8]	0.0691[1.5]	0.0804[5]	0.0804[5]	0.0893[7]	0.0804[5]	0.0691[1.5]	0.0692[3]

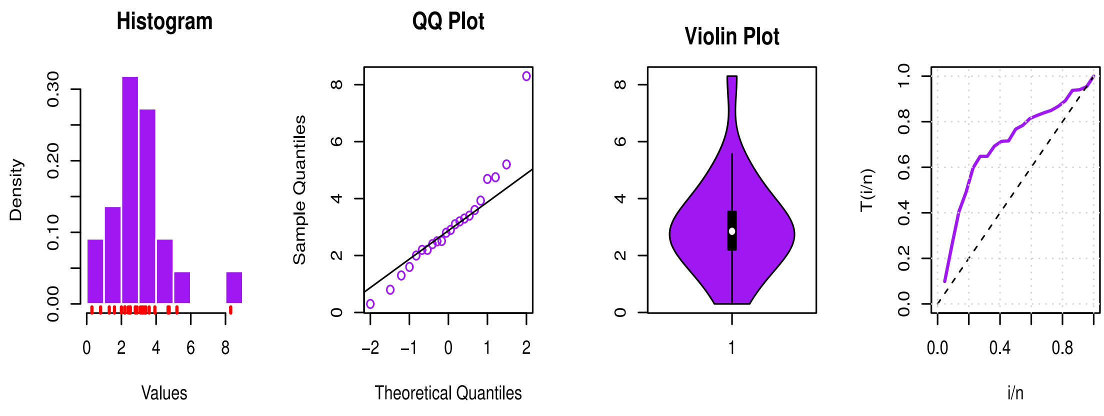

Fig. 5. Some basic non-parametric plots for the dataset 1.

the histogram of the data sets with the fitted PDFs forms the eight estimation methods displayed in Figs. 11–23, The CDFs and the fitted densities in Figs. 12–24, and PP and the fitted densities in Figs. 13–25.

Summary & discussion

In recent years, there has been a surge in the development of novel, adaptable probability distributions. These distributions, often derived from existing ones, aim to enhance their applicability across various domains. This study introduces the transmuted power Chris-Jerry distribution as a new lifetime distribution. This distribution is a member of the Transmuted-G family and extends

Table 10
Partial and overall ranks for tables from Tables 4 to 9.

Parameters	n	MLE	ADE	CME	LSE	RADE	WLSE	ADLTSE	PE
$\eta = 0.4,\ \kappa = 0.8$ and $\tau = 0.9$	30	3	2	7	6	5	8	4	1
	50	1	4.5	7	7	2.5	7	4.5	2.5
	150	5	1.5	7	7	3	7	1.5	4
	300	5	3.5	7	7	1.5	7	3.5	1.5
	450	5	3	7	7	1	7	3	3
$\eta = 0.8,\ \kappa = 1.2$ and $\tau = 0.3$	30	1	7	3	6	2	5	4	8
	50	2	7	4	4	1	4	6	8
	150	3.5	6.5	3.5	3.5	1	3.5	6.5	8
	300	2	6.5	4	4	1	4	6.5	8
	450	1	6.5	4	4	2	4	6.5	8
$\eta = 0.8,\ \kappa = 1.9$ and $\tau = 0.9$	30	2.5	1	7	5.5	5.5	8	4	2.5
	50	3.5	5	7	6	3.5	8	2	1
	150	5	2.5	7	7	1	7	2.5	4
	300	5	3	7	7	1	7	3	3
	450	8	2.5	5	6.5	1	6.5	2.5	4
$\eta = 1.4,\ \kappa = 0.4$ and $\tau = 0.3$	30	1	8	3	6	2	4.5	7	4.5
	50	1	5	7	7	2	7	4	3
	150	1	6.5	3	3	5	3	6.5	8
	300	1	3	7	7	5	7	3	3
	450	1	3	7	7	5	7	3	3
$\eta = 1.4,\ \kappa = 0.4$ and $\tau = 0.7$	30	1	2	7	6	3	8	4	5
	50	1	3	6.5	6.5	5	8	2	4
	150	4.5	1.5	7	7	3	7	1.5	4.5
	300	4	2	7	7	5	7	2	2
	450	8	3	6	6	1	6	3	3
$\eta = 2,\ \kappa = 0.8$ and $\tau = 0.7$	30	1	3.5	8	5	3.5	7	6	2
	50	2	5	7	7	1	7	4	3
	150	5	2.5	7	7	1	7	2.5	4
	300	5.5	2	5.5	5.5	8	5.5	2	2
	450	5.5	1.5	5.5	5.5	8	5.5	1.5	3
$\sum$ Ranks		95	113.5	180	180	89.5	189.5	112	120.5
Overall ranks		2	4	6.5	6.5	1	8	3	5

Table 11
Inflation rate which recorded in Jun 2024.

Country	Inflation rate %	Country	Inflation rate %	Country	Inflation rate %	Country	Inflation rate %
Australia	3.60	Germany	2.20	Netherlands	3.20	Spain	3.40
Brazil	3.93	India	4.75	Russia	8.30	Switzerland	1.30
Canada	2.90	Indonesia	2.51	United Kingdom	2.00	Saudi Arabia	1.60
China	0.30	Italy	0.80	Singapore	3.10	United States	3.30
Euro Area	2.50	South Africa	5.20	Japan	2.80		
France	2.20	Mexico	4.69	South Korea	2.40		

Table 12
Some descriptive analysis of all data sets.

	n	μ_1'	Median	σ^2	σ	λ_1	λ_2	Range	Min	Max	Sum
data1	22	3.0445	2.850	2.8805	1.6972	1.219	5.407	8.000	0.300	8.300	66.980
data2	128	9.2094	6.280	108.21	10.405	3.399	19.394	78.970	0.080	79.050	1178.8
data3	211	4.582	2.770	31.867	5.645	2.594	11.568	36.990	0.030	37.020	966.88

the two-parameter PCJD. The Tr-PCJD, a versatile extension of the PCJD, offers a simple yet effective approach to modeling non-negative real-world data. Its hazard rate function, capable of exhibiting various shapes such as increasing, decreasing, J-shaped, and reversed J-shaped, underscores its adaptability. Similarly, the density function can accommodate reverse J, left- or right-skewed, or symmetrical data. In particular, it encompasses the CJD, PCJD, and transmuted CJD. To delve into its significance, we explore its mathematical properties, including random number generation, Bowley's skewness, Moor's kurtosis, moments, incomplete moments, and extropy measures. Moreover, we investigate eight estimation techniques for its unknown parameters. However, the applicability of Tr-PCJD is demonstrated through its application to three real-world datasets from various fields. It consistently outperforms several competing distributions in terms of model fit. A comprehensive simulation study evaluates the performance of the estimators CM, ML, RTAD, LS, percentiles, AD, WLS, and ADLTS. The following conclusions are drawn in light of the numerical results and real data analysis:

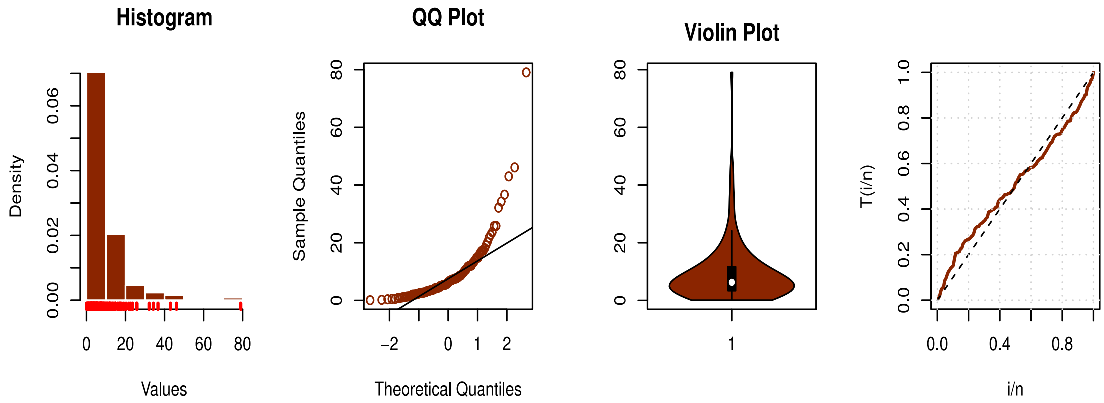

Fig. 6. Some basic non-parametric plots for the dataset 2.

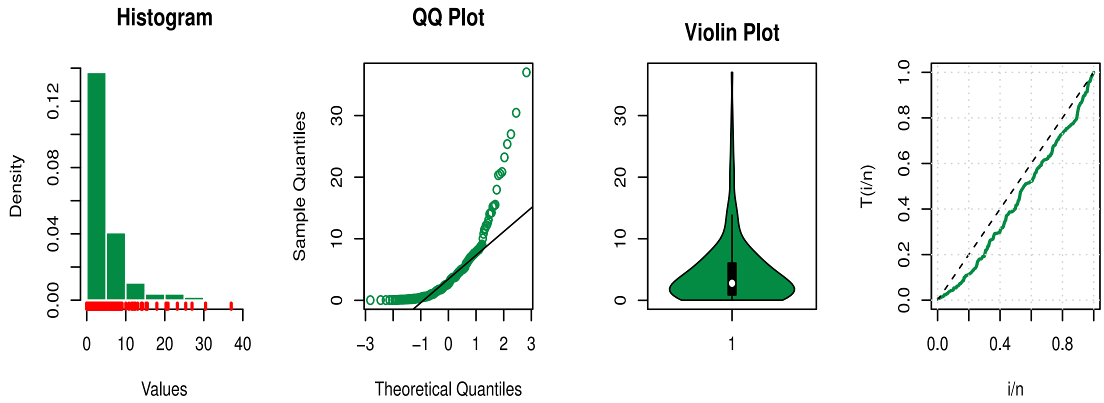

Fig. 7. Some basic non-parametric plots for the dataset 3.

Table 13
MLEs and (SEs) for competitive models to the data set 1.

Models	$\hat{\kappa}$	$\hat{\eta}$	$\hat{\tau}$	$\hat{\theta}$	SE($\hat{\kappa}$)	SE($\hat{\eta}$)	SE($\hat{\tau}$)	SE($\hat{\theta}$)
Tr-PCJD	1.4385	0.3805	0.6868		0.1954	0.1111	0.4152	
XLD	0.4758				0.0756			
PCJD	0.5288	1.3682			0.1413	0.1855		
KwCJD	0.9559	1.9995	1.2942		0.6751	0.8621	1.6520	
EGXLD	59.2893	0.0505	2.0251		243.7637	0.1162	0.7654	
KwLD	0.3463	1.7807	4.1649		0.4822	0.8894	9.8057	
WPLD	0.0200	1.0710	13.3755	61.8533	0.0187	0.0923	23.0746	55.0031
WLD	1.9006	0.2919	0.0002		0.3030	0.0345	0.7661	

Table 14
Fitting measures values for the data set 1.

Name	W_1	W_2	W_3	W_4	W_5	W_6	W_7	W_8	W_9
Tr-PCJD	86.2205	87.5539	86.9916	0.0953	0.9884	0.0361	0.9557	0.2482	0.9712
XLD	92.0141	92.2141	92.2711	0.2634	0.0945	0.3685	0.0869	1.8797	0.1076
PCJD	87.9378	88.5694	88.4518	0.1084	0.9584	0.0482	0.8916	0.3166	0.9244
KwCJD	86.5839	87.9172	87.3550	0.1097	0.9539	0.0417	0.9284	0.2784	0.9531
EGXLD	87.2359	88.5692	88.0069	0.1206	0.9060	0.0519	0.8695	0.3383	0.9059
KwLD	87.1021	88.4354	87.8731	0.1176	0.9211	0.0487	0.8888	0.3199	0.9217
WPLD	89.5916	91.9445	90.6197	0.1234	0.8913	0.0610	0.8127	0.3839	0.8632
WLD	87.5766	88.9099	88.3476	0.1229	0.8937	0.0603	0.8170	0.3811	0.8660

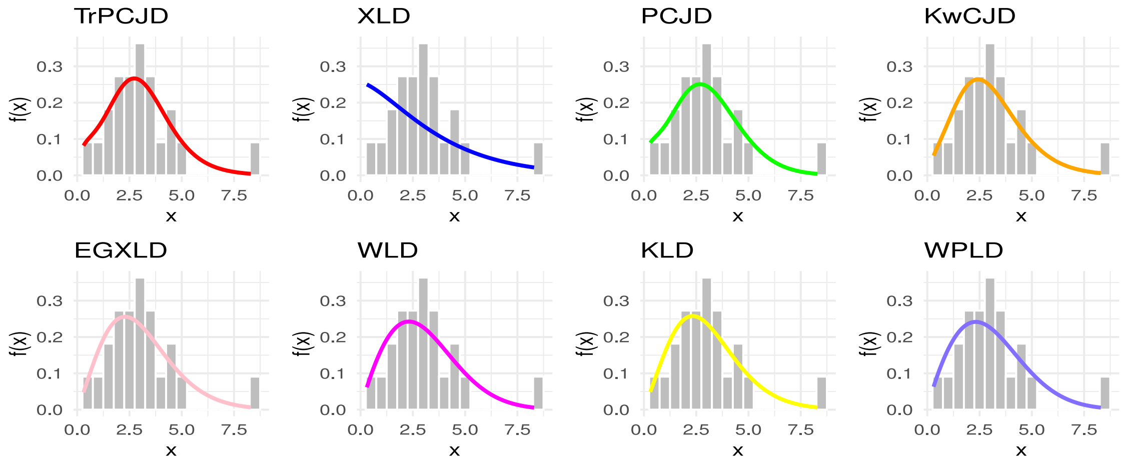

Fig. 8. Estimated PDFs for the dataset 1.

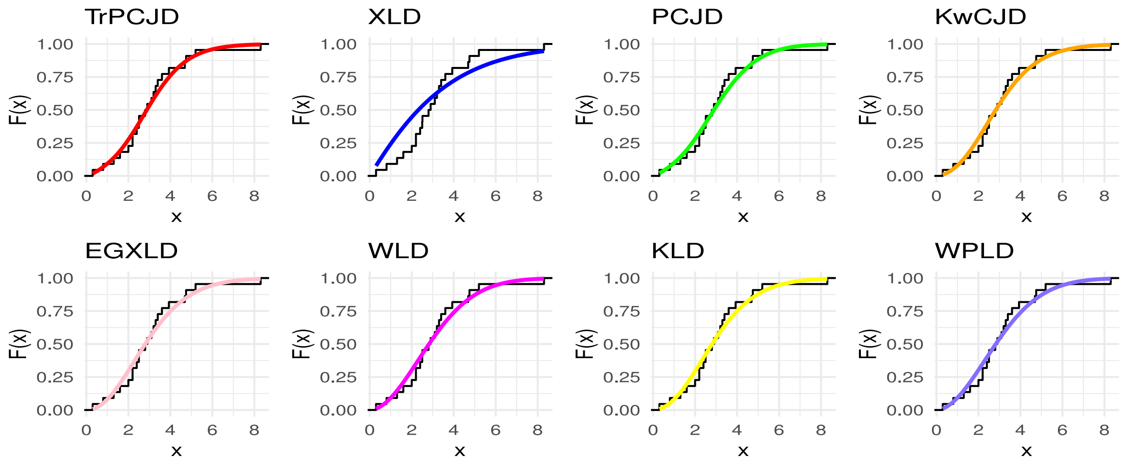

Fig. 9. Estimated CDFs for the dataset 1.

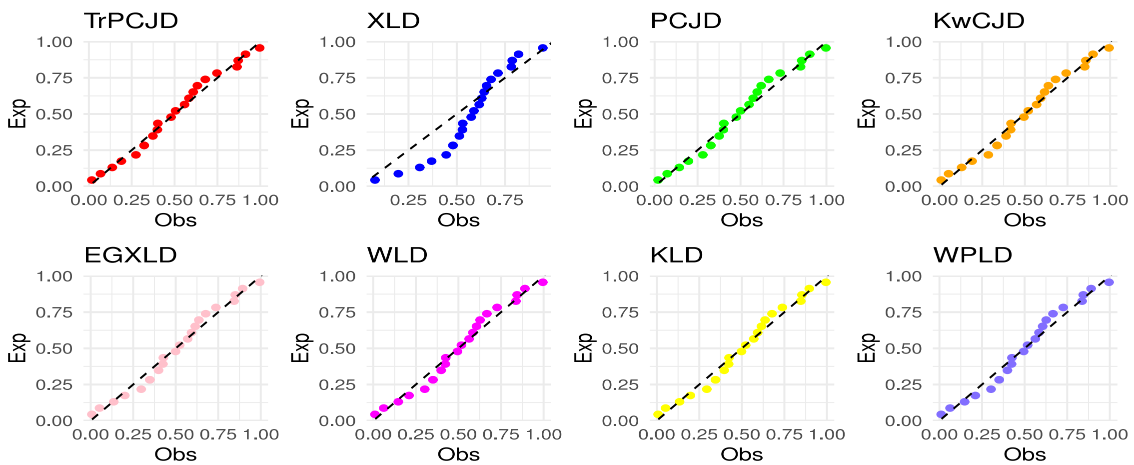

Fig. 10. PP plots for the dataset 1.

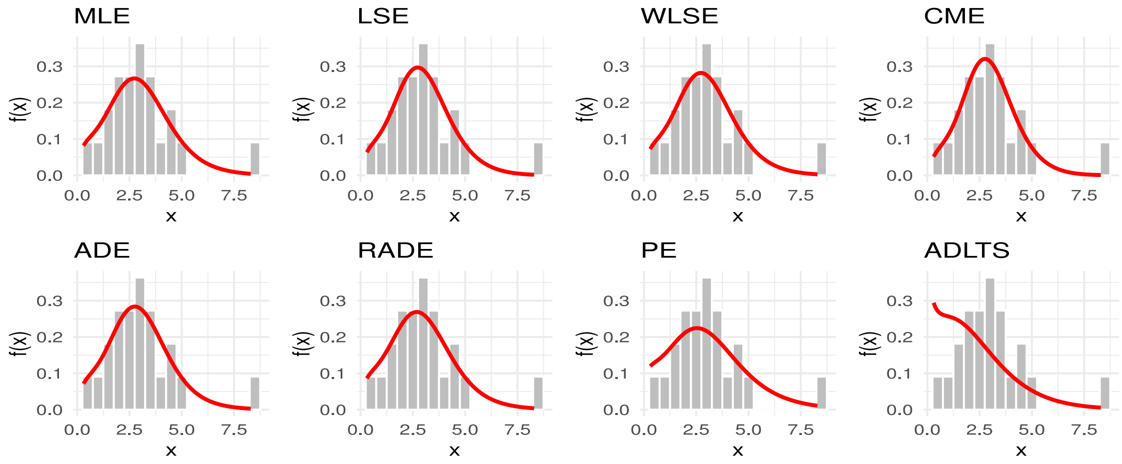

Fig. 11. Estimated PDFs using different estimation methods for the dataset 1.

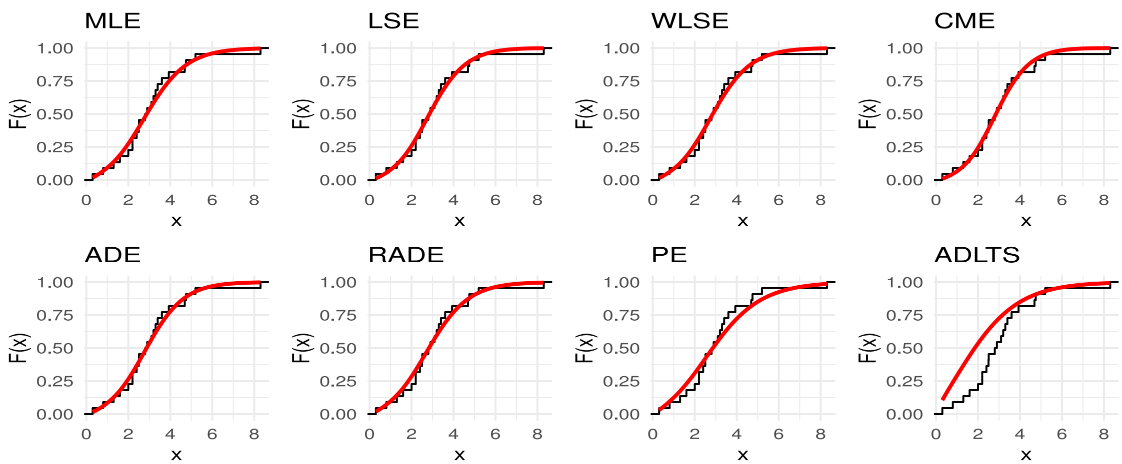

Fig. 12. Estimated CDFs using different estimation methods for the dataset 1.

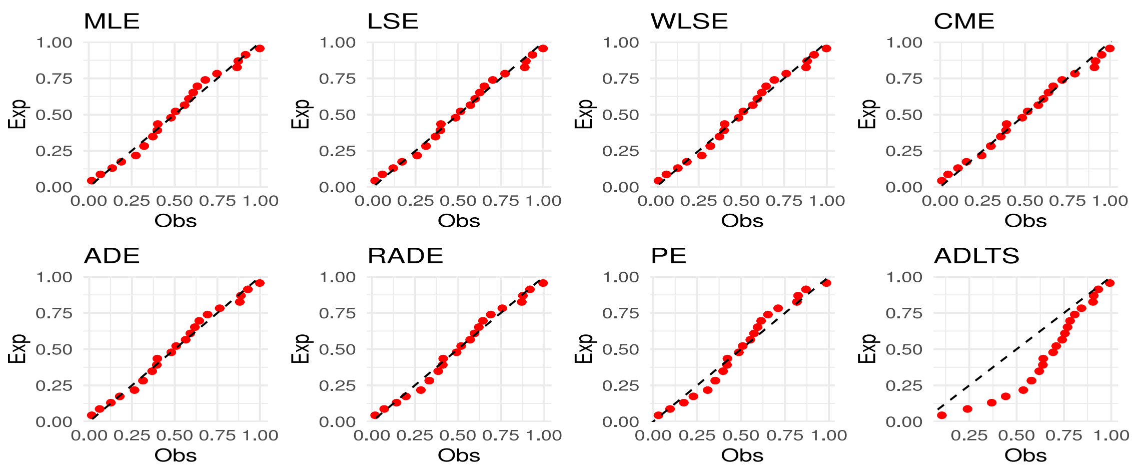

Fig. 13. The PP plots using different estimation methods for the dataset 1.

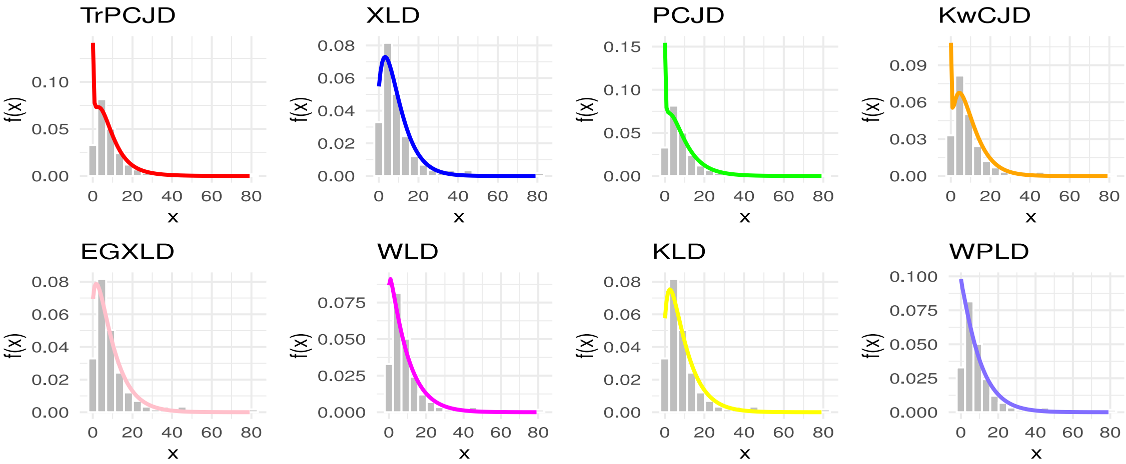

Fig. 14. Estimated PDFs for the dataset 2.

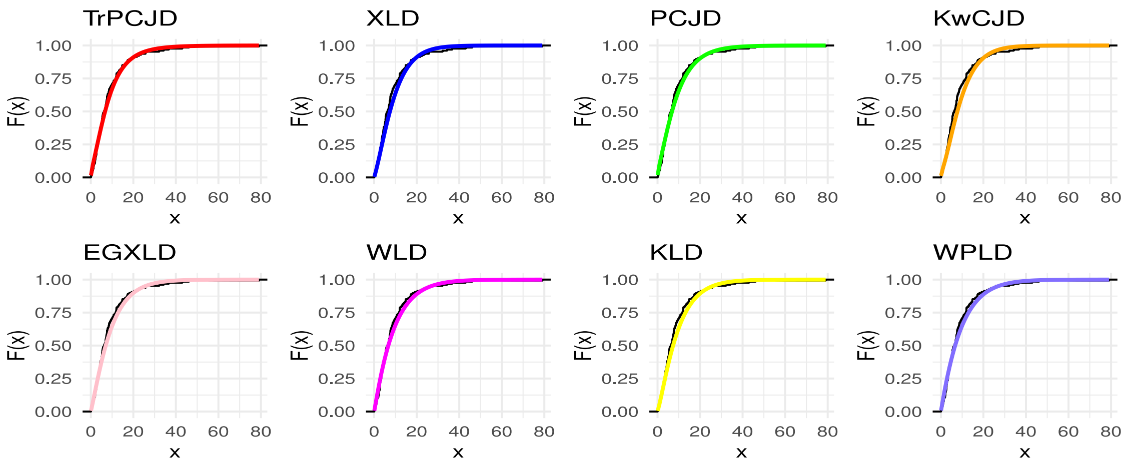

Fig. 15. Estimated CDFs for the dataset 2.

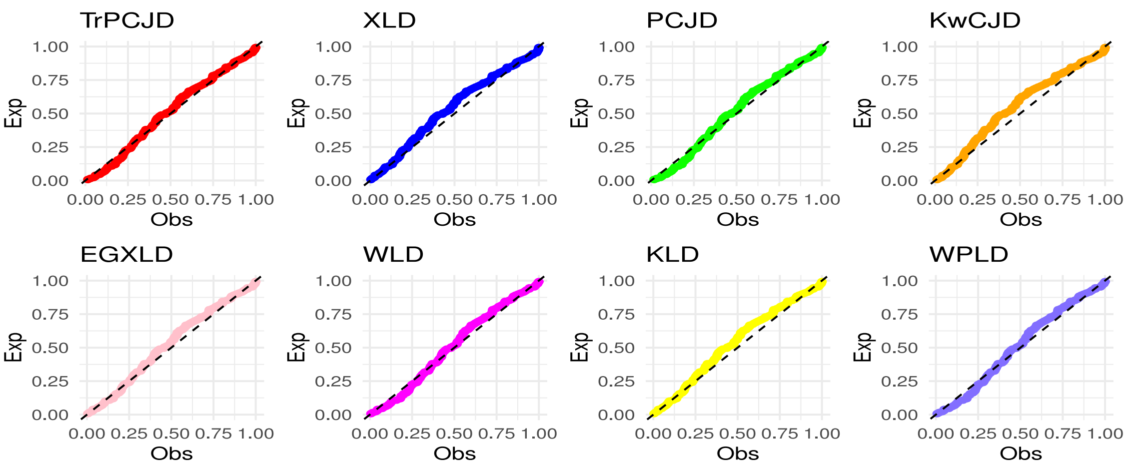

Fig. 16. PP plots for the dataset 2.

Table 15
MLEs, W_4 and W_5 using eight estimation methods for the data set 1.

Models	$\hat{\kappa}$	$\hat{\eta}$	$\hat{\tau}$	W_4	W_5
MLE	1.4385	0.3805	0.6868	0.0953	0.9884
LSE	1.5724	0.3589	0.5486	0.0839	0.9978
WLSE	1.5063	0.3723	0.6026	0.0909	0.9933
CME	1.6709	0.3285	0.5452	0.0909	0.9933
ADE	1.5065	0.3567	0.706	0.0874	0.9961
RADE	1.4302	0.3877	0.7157	0.1068	0.9632
PE	1.2501	0.4703	0.5881	0.1283	0.862
ADLTSE	0.9191	1.2069	−0.2124	0.3536	0.0082

Table 16
MLEs and (SEs) for competitive models to the data set 2.

Models	$\hat{\kappa}$	$\hat{\eta}$	$\hat{\tau}$	$\hat{\theta}$	SE($\hat{\kappa}$)	SE($\hat{\eta}$)	SE($\hat{\tau}$)	SE($\hat{\theta}$)
Tr-PCJD	0.7773	0.3984	0.6572		0.0432	0.0497	0.2099	
XLD	0.1859				0.0118			
PCJD	0.5443	0.7419			0.0588	0.0409		
KwCJD	0.5368	0.6983	0.3330		0.0029	0.1140	0.0330	
EGXLD	0.2916	0.4800	1.0244		0.0345	0.0056	0.1218	
KwLD	0.5015	0.9518	0.2795		0.0028	0.1661	0.0273	
WPLD	0.0429	1.1229	0.0844	15.1898	0.0345	0.0592	0.1337	12.5986
WLD	1.0515	0.1062	0.0000		0.0675	0.0094	0.0159	

Table 17
Fitting measures values for the data set2.

Name	W_1	W_2	W_3	W_4	W_5	W_6	W_7	W_8	W_9
Tr-PCJD	829.3099	829.5035	832.7863	0.0649	0.6545	0.1183	0.5028	0.8655	0.4359
XLD	831.9418	831.9736	833.1006	0.1017	0.1415	0.3348	0.1081	1.7385	0.1286
PCJD	830.8459	830.9419	833.1635	0.0743	0.4801	0.1712	0.3313	1.1796	0.2754
KwCJD	839.7437	839.9372	843.2201	0.1220	0.0444	0.5369	0.0320	2.6621	0.0409
EGXLD	829.7563	829.9498	833.2327	0.0852	0.3104	0.1902	0.2875	1.0352	0.3392
KwLD	829.5787	829.7722	833.0550	0.1003	0.1518	0.3078	0.1285	1.5033	0.1757
WPLD	831.9937	832.3189	836.6289	0.0712	0.5355	0.1641	0.3497	1.0455	0.3341
WLD	829.7849	829.9785	833.2613	0.0720	0.5208	0.1661	0.3444	1.0471	0.3333

Table 18
MLEs, W_4 and W_5 using eight estimation methods for the data set 2.

Models	$\hat{\kappa}$	$\hat{\eta}$	$\hat{\tau}$	W_4	W_5
MLE	0.7773	0.3984	0.6572	0.0649	0.6545
LSE	0.8418	0.3994	0.4541	0.0536	0.8555
WLSE	0.8445	0.3868	0.4854	0.0485	0.9241
CME	0.8501	0.3946	0.4511	0.0511	0.8916
ADE	0.8194	0.3885	0.5724	0.0550	0.8328
RADE	0.7633	0.4246	0.6301	0.0790	0.4009
PE	0.5685	0.6182	0.7689	0.2034	0.0001
ADLTSE	0.6629	0.7530	0.4714	0.2662	0.0000

Table 19
MLEs and (SEs) for competitive models to the data set 3.

Models	$\hat{\kappa}$	$\hat{\eta}$	$\hat{\tau}$	$\hat{\theta}$	SE($\hat{\kappa}$)	SE($\hat{\eta}$)	SE($\hat{\tau}$)	SE($\hat{\theta}$)
Tr-PCJD	0.6933	0.7381	0.6188		0.0332	0.0861	0.2479	
XLD	0.3413				0.0171			
PCJD	0.9859	0.6583			0.0668	0.0312		
KwCJD	0.1848	0.5101	2.3963		0.1864	0.0484	3.1119	
EGXLD	0.1895	1.0443	0.7084		0.0190	0.0027	0.0608	
KLD	0.0288	0.5279	10.1773		0.0332	0.0315	12.1599	
WPLD	0.0769	0.9695	2.0048	7.0948	0.1392	0.3604	3.4430	12.5117
WLD	0.8319	0.2411	0.0000		0.0445	0.0210	0.0677	

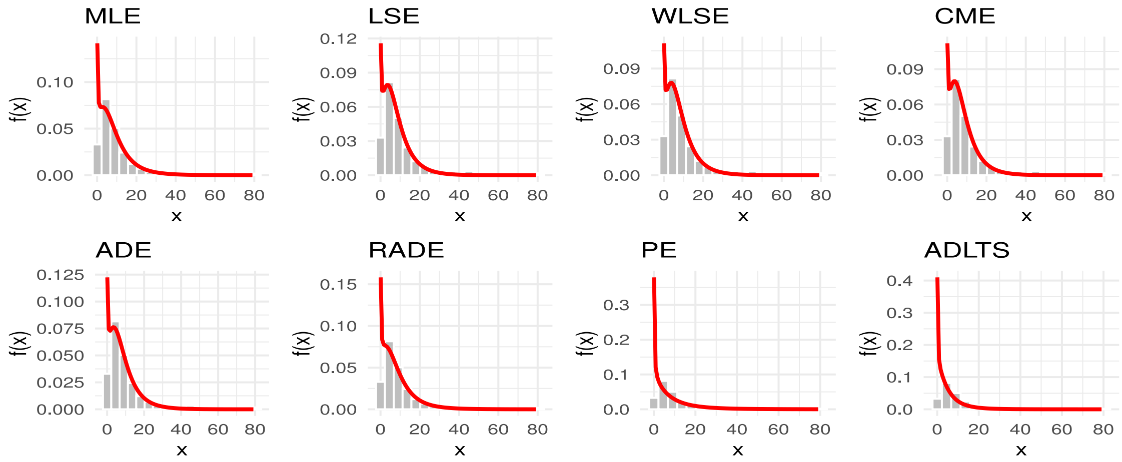

Fig. 17. Estimated PDFs using different estimation methods for the dataset 2.

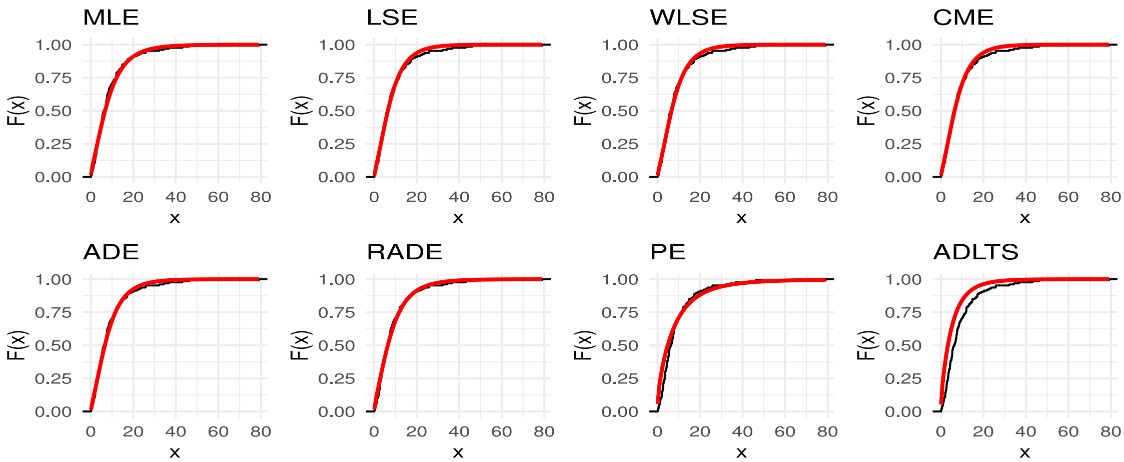

Fig. 18. Estimated CDFs using different estimation methods for the dataset 2.

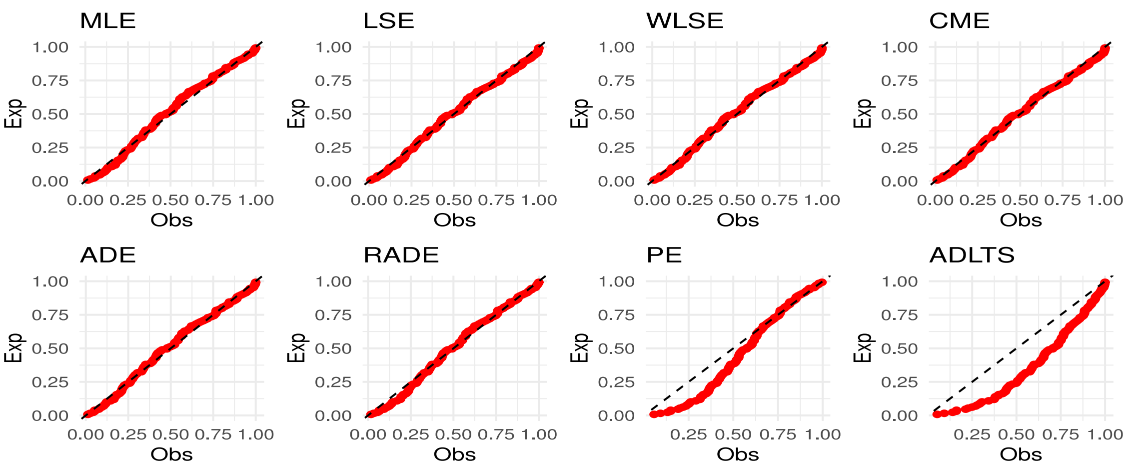

Fig. 19. The PP plots using different estimation methods for the dataset 2.

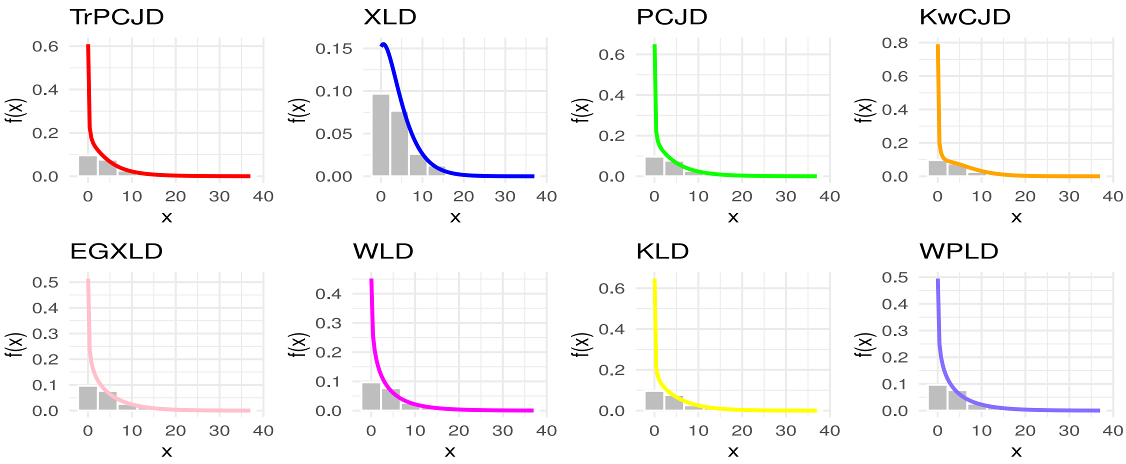

Fig. 20. Estimated PDFs for the dataset 3.

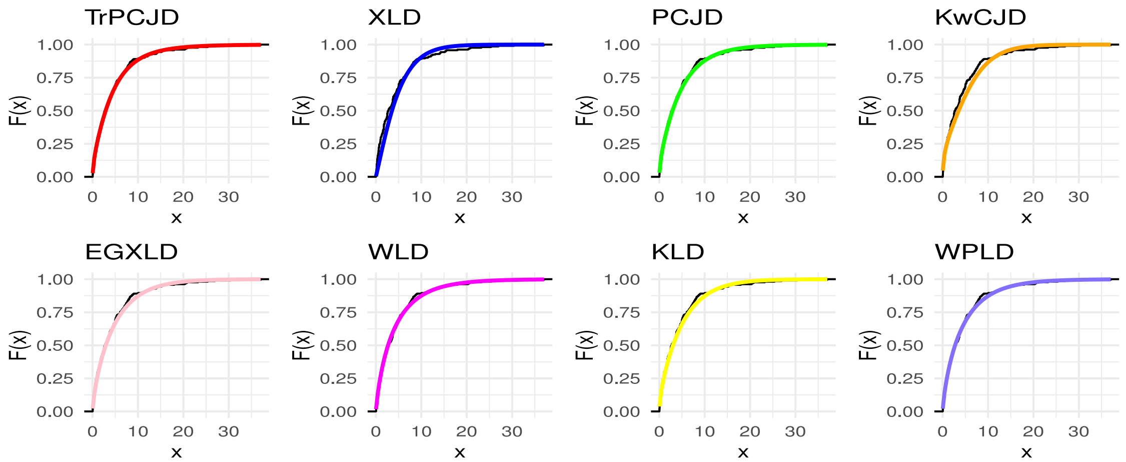

Fig. 21. Estimated CDFs for the dataset 3.

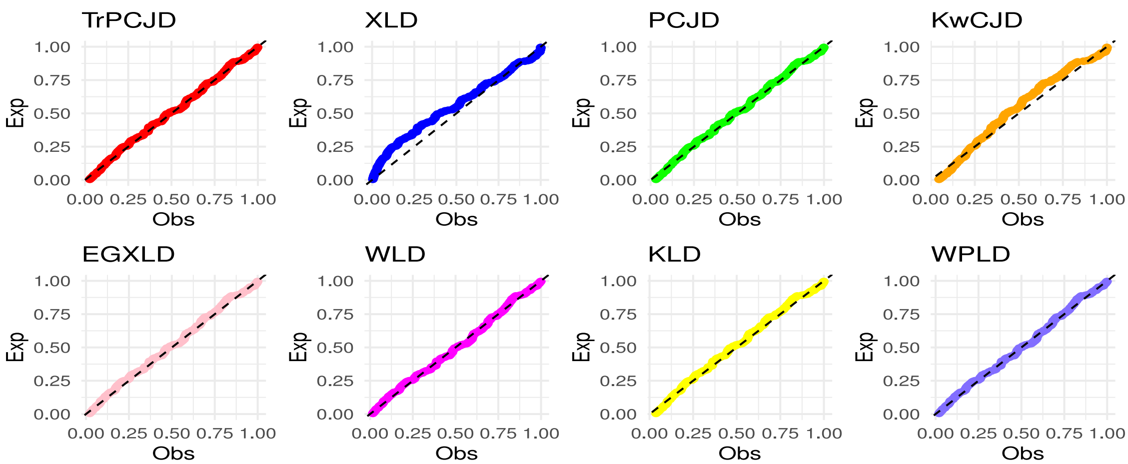

Fig. 22. PP plots for the dataset 3.

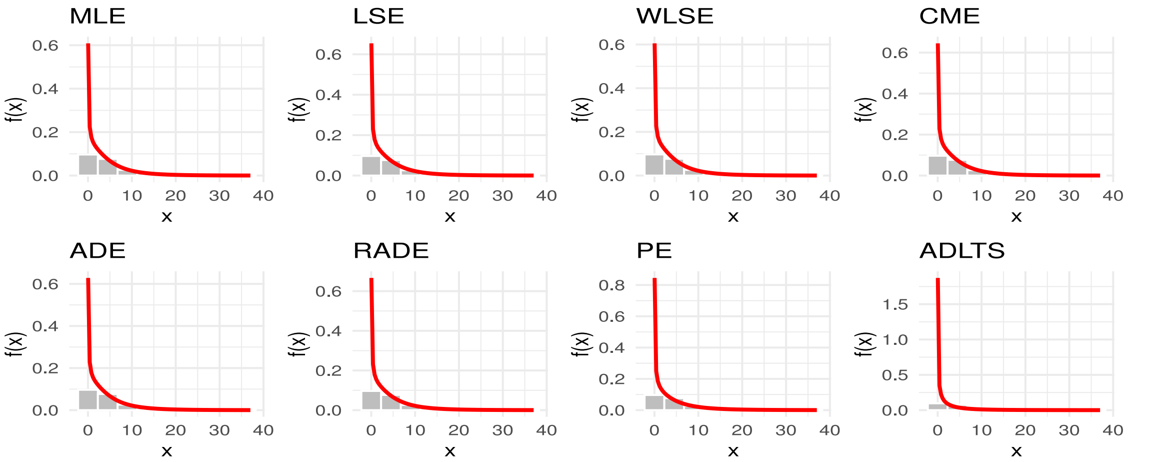

Fig. 23. Estimated PDFs using different estimation methods for the dataset 3.

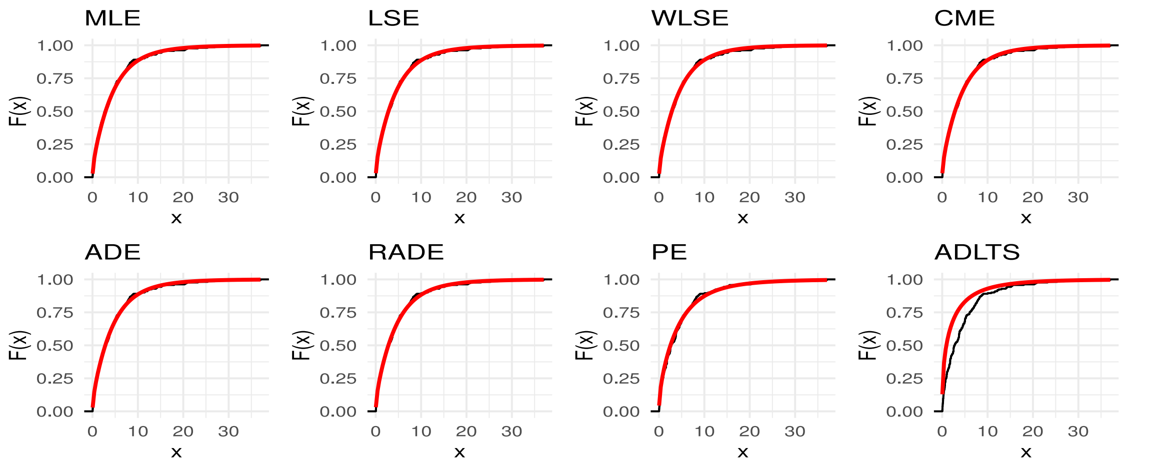

Fig. 24. Estimated CDFs using different estimation methods for the dataset 3.

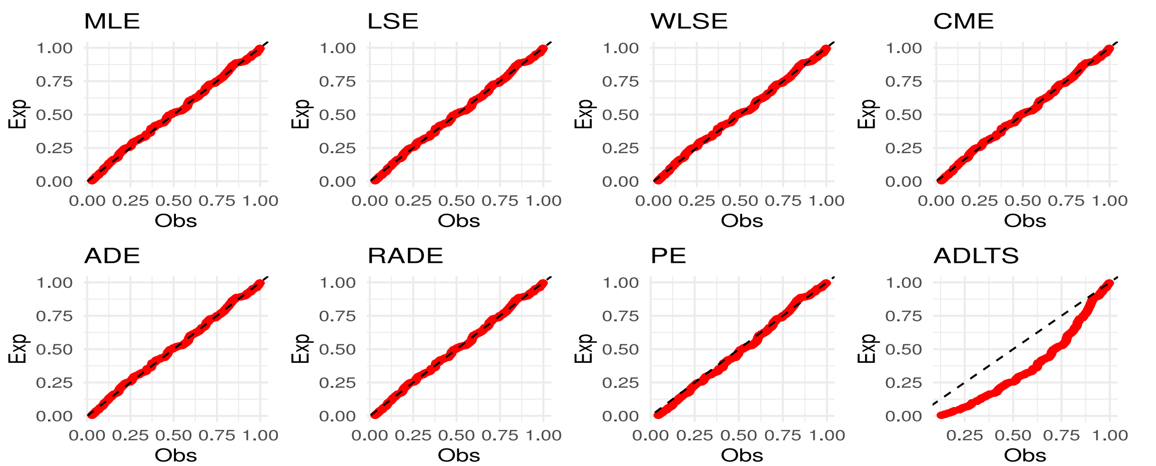

Fig. 25. The PP plots using different estimation methods for the dataset 3.

Table 20
Fitting measures values for the data set3.

Name	W_1	W_2	W_3	W_4	W_5	W_6	W_7	W_8	W_9
Tr-PCJD	1060.1200	1060.2360	1064.1850	0.0329	0.9765	0.0413	0.9266	0.3321	0.8162
XLD	1095.0270	1095.0460	1096.3820	0.1350	0.0009	1.1482	0.0011	8.8448	<0.0001
PCJD	1060.8020	1060.8600	1063.5120	0.0382	0.9177	0.0523	0.8625	0.5636	0.6828
KwCJD	1088.4400	1088.5560	1092.5050	0.0896	0.0674	0.4691	0.0477	3.0032	0.0273
EGXLD	1060.1900	1060.3060	1064.2550	0.0459	0.7660	0.0709	0.7466	0.5743	0.6724
KLD	1068.7590	1068.8750	1072.8240	0.0472	0.7340	0.0998	0.5862	0.9051	0.4110
WPLD	1060.6640	1060.8580	1066.0830	0.0423	0.8443	0.0475	0.8917	0.3905	0.7580
WLD	1060.3330	1060.4490	1064.3980	0.0387	0.9106	0.0543	0.8506	0.3839	0.8044

Table 21
MLEs, W_4 and W_5 using eight estimation methods for the data set 3.

Models	$\hat{\kappa}$	$\hat{\eta}$	$\hat{\tau}$	W_4	W_5
MLE	0.6933	0.7381	0.6188	0.0329	0.9765
LSE	0.6748	0.7215	0.7487	0.0316	0.9842
WLSE	0.6999	0.7532	0.5741	0.0317	0.9839
CME	0.6788	0.7178	0.7525	0.0309	0.9876
ADE	0.6890	0.7489	0.6179	0.0296	0.9927
RADE	0.6720	0.7443	0.6836	0.0327	0.9780
PE	0.6149	0.8074	0.7020	0.0534	0.5848
ADLTSE	0.4937	1.4113	0.4327	0.2662	0.0000

- The RTAD method consistently followed by the ML method outperforms the others. Consequently, the RTAD method is recommended for estimating the Tr-PCJD parameters.
- The consistency of all estimate techniques is demonstrated by the observed decline in MSE with increasing sample size.
- In terms of rank, MLE is the second-best approach, successed by the ADE and ADLTS.
- The Tr-PCJD outperformed a number of LD extensions and generalizations in the actual data application. The use of real-world datasets with a variety of features, which enabled a comprehensive assessment of the Tr-PCJD's wide applicability in many contexts, corroborated this strong conclusion.

This rigorous approach underscores both the practical relevance and potential limitations of the distribution in real-world contexts. In order to overcome this article's drawback, future research should go beyond complete samples and examine both classical and Bayesian parameter estimation for the new distribution under different censoring schemes.

CRediT authorship contribution statement

Mohammed Elgarhy: Writing – original draft, Validation, Methodology, Formal analysis, Conceptualization, Writing – review, Investigation. **Diaa S. Metwally:** Writing – original draft, Validation, Methodology, Formal analysis, Conceptualization, Writing-review, Investigation. **Amal S. Hassan:** Writing – original draft, Validation, Methodology, Formal analysis, Conceptualization, Writing-review, Investigation. **Ahmed W. Shawki:** Writing – original draft, Validation, Methodology, Formal analysis, Conceptualization, Writing – review, Investigation.

Consent for publication

All the authors agreed to publish this research.

Ethics approval and consent to participate

Ethics approval and consent to participate.

Funding statement

This work was supported and funded by the Deanship of Scientific Research at Imam Mohammad Ibn Saud Islamic University (IMSIU) (grant number IMSIU-DDRSP2503).

Declaration of competing interest

The authors declare that they have no known competing financial interests or personal relationships that could have appeared to influence the work reported in this paper.

Acknowledgments

This work was supported and funded by the Deanship of Scientific Research at Imam Mohammad Ibn Saud Islamic University (IMSIU) (grant number IMSIU-DDRSP2503).

Data availability

The data that support the findings of this study are available on request from the corresponding author. The data are not publicly available due to privacy or ethical restrictions.

References

[1] N. Eugene, C. Lee, F. Famoye, Beta-normal distribution and its applications, Comm. Statist. Theory Methods 31 (2002) 497–512.
[2] G.M. Cordeiro, M. de Castro, A new family of generalized distributions, J. Stat. Comput. Simul. 81 (2011) 883–898.
[3] M. Bourguignon, R.B. Silva, G.M. Cordeiro, The Weibull-G family of probability distributions, J. Data Sci. 12 (2014) 53–68.
[4] A. Al-Shomrani, O. Arif, A. Shawky, S. Hanif, M.Q. Shahbaz, Topp-leone family of distributions: Some properties and application, Pak. J. Stat. Oper. Res. 12 (2016) 443–451.
[5] A. Algarni, A.M. Almarashi, I. Elbatal, A.S. Hassan, E.M. Almetwally, A.M. Daghistani, M. Elgarhy, Type I half logistic burr X-G family: Properties, Bayesian, Non- Bayesian Estim. under Censored Samples Appl. To COVID- 19 Data. Math. Probl. Eng. 5461130 (21) (2021) http://dx.doi.org/10.1155/2021/5461130.
[6] A. Alghamdi, M.M. Abd El-Raouf, Exploring the dynamics of COVID-19 with a novel family of models, Math. 11 (2023) 1641, http://dx.doi.org/10.3390/math11071642.
[7] J.T. Eghwerido, L.C. Nzei, A.E. Omotoye, F.I. Agu, The Teissier-G family of distributions: Properties and applications, Math. Slovaca 72 (2022) 1301–1318.
[8] A.S. Hassan, N. Alsadat, C. Chesneau, A.W. Shawki, A novel weighted family of probability distributions with applications to world natural gas, oil, and gold reserves, Math. Biosci. Eng. (MBE) 20 (11) (2023) 19871–19911, http://dx.doi.org/10.3934/mbe.2023880.
[9] A.S. Hassan, M. Sabry, A, A.M. Elsehetry, A new family of upper-truncated distributions: Properties and estimation, Thail. Stat. 18 (2) (2020) 196–214.
[10] A.Z. Afify, G.M. Cordeiro, N.A. Ibrahim, F. Jamal, M. Elgarhy, M.A. Nasir, The Marshall–Olkin odd burr III-g family: Theory, estimation, and engineering applications, IEEE Access 9 (2021) 4376–4387, http://dx.doi.org/10.1109/ACCESS.2020.3044156.
[11] Y.Y. Abdelall, A.S. Hassan, E.M. Almetwally, A new extention of the odd inverse Weibull-g family of distributions: Bayesian and non-Bayesian estimation with engineering applications, Comput. J. Math. Stat. Sci. 3 (2) (2024) 359–388, http://dx.doi.org/10.21608/CJMSS.2024.285399.1050.
[12] M.N. Atchade, A.A. Agbahide, T. Otodji, M.J. Bogninou, A.Moussa. Djibril, A new shifted lomax-x family of distributions : Properties and applications to actuarial and financial data, Comput. J. Math. Stat. Sci. 4 (1) (2025) 41–71, http://dx.doi.org/10.21608/cjmss.2024.307114.1066.
[13] Shaw. WT, IRC. Buckley, The alchemy of probability distributions: beyond gram–charlier expansions, and a skew-kurtotic-normal distribution from a rank transmutation map, 2009, ArXiv e-prints.
[14] N. Helmy, Transmuted Burr type II distribution, Egyptian Statist. J. 61 (2) (2017) 58–68, http://dx.doi.org/10.21608/esju.2017.270086.
[15] S.M. Mohamed, M.M. Mansour, A new generalization of the Pareto distribution: With application, Egyptian Statist. J. 59 (1) (2015) 108–126, http://dx.doi.org/10.21608/esju.2015.314459.
[16] A.S. Hassan, M.A. Khaleel, S.G. Nassr, Transmuted topp-leone power function distribution: Theory and application, J. Stat. Appl. Probab. 10 (1) (2021) 215–227, http://dx.doi.org/10.18576/jsap/100120.
[17] A.S. Hassan, S.M. Assar, A.M. Abd Elghaffar, Statistical properties and estimation of power-transmuted inverse Rayleigh distribution, Stat. Transit. New Ser. 21 (3) (2020) 1–20.
[18] M. Elgarhy, I. Elbatal, M.A. ul Haq, A.M. Hassan, Transmuted kumaraswamy quasi lindley distribution with applications, Ann. Data Sci. 5 (4) (2018) 565–581, http://dx.doi.org/10.1007/s40745-018-0153-4.
[19] C.K. Onyekwere, O.J. Obulezi, Chris-jerry distribution and its applications, Asian J. Probab. Stat. 20 (1) (2022) 16–30.
[20] I.C. Obulezi O.J, O.G. Oyo, H.O. Etaga, Marshall–olkin chris-jerry distribution and its applications, Int. J. Innov. Sci. Res. Technol. 8 (5) (2023) 522-433.
[21] C.F. Innocent, O.A. Frederick, E.M. Udofia, O.J. Obulezi, Estimation of the parameters of the power size biased chris-jerry distribution, Int. J. Innov. Sci. Res. Technol. 8 (5) (2023) 423–436.
[22] C.I. Ezeilo, O.I. Sidney, E.U. Umeh, C.K. Onyekwere, On power chris-jerry distribution: Properties and parameter estimation methods, Asian J. Probab. Stat. 25 (3) (2023) 29–44.
[23] O. Obulezi, J. Anabike, C. Ifeanyi, G.C. Okoye, C.P. Igbokwe, H.O. Etaga, C.K. Onyekwere, The kumaraswamy chris-jerry distribution and its applications, J. Xidian Univ. 17 (6) (2023) 575–591.
[24] D.O. Oramulu, C.P. Igbokwe, I.C. Anabike, H.O. Etaga, O.J. Obulezi, Simulation study of the Bayesian and non-Bayesian estimation of a new lifetime distribution parameters with increasing hazard rate, Asian Res. J. Math. 19 (9) (2023) 183–211.
[25] E.Q. Chinedu, Q.C. Chukwudum, N. Alsadat, O.J. Obulezi, E.M. Almetwally, A.H. Tolba, New lifetime distribution with applications to single acceptance sampling plan and scenarios of increasing hazard rates, Symmetry 15 (2023) 1881, http://dx.doi.org/10.3390/sym15101881.
[26] F. LAD, G. SANFILIPPO, Extropy: Complementary dual of entropy, Statist. Sci. 30 (1) (2015) 40–58.
[27] R.A. Fisher, On the mathematical foundations of theoretical statistics, Philos. Trans. R. Soc. Lond. Ser. A 222 (594–604) (1922) 309–368.
[28] Fisher, R. A, Theory of statistical estimation, in: Mathematical Proceedings of the Cambridge Philosophical Society, Vol. 22, Cambridge University Press, 1925, pp. 700–725, (5).
[29] T.W. Anderson, D.A. Darling, Asymptotic theory of certain goodness of fit criteria based on stochastic processes, Ann. Math. Stat. 19 (1952) 3–212.
[30] K. Choi, W.G. Bulgren, An estimation procedure for mixtures of distributions, J. R. Stat. Soc. Ser. B Stat. Methodol. 30 (3) (1968) 444–460.
[31] J. Swain, V. Sekhar, R.W. James, Least-squares estimation of distribution functions in johnson's translation system, J. Stat. Comput. Simul. 29 (4) (1988) 271–297.
[32] E.T. Lee, J.W. Wang, Statistical Methods for Survival Data Analysis, 3rd ed., John Wiley and Sons, New York, NY, USA, 2003.
[33] A.S. Hassan, A.W. Shawki, H.Z. Muhammeda, Weighted Weibull-G family of distributions: Theory & application in the analysis of renewable energy sources, J. Posit. Sch. Psychol. 6 (3) (2022) 9201–9216.
[34] S. Chouia, H. Zeghdoudi, The xlindley distribution: properties and application, J. Stat. Theory Appl. 20 (2) (2021) 318–327.
[35] S. Abdelmoezz, S.M. Mohamed, The kumaraswamy lindley regression model with application on the Egyptian stock exchange: Numerical study, regression model, J. Mat. Stat. Dan Komputasi 18 (1) (2021) 1–11.
[36] M. Bourguignon, R.B. Silva, G.M. Cordeiro, The Weibull-G family of probability distributions, J. Data Sci. 12 (1) (2014) 53–68.
[37] A.K.B.A.R. Asgharzadeh, S. Nadarajah, F. Sharafi, Weibull Lindley distribution, Revstat- Stat. J. 16 (1) (2018) 87–113.
[38] R.R. MusEGPLDa, B. Makubate, A flexible generalized xlindley distribution with application to engineering, Sci. Afr. 24 (2024) e02192.